RESEARCH and

TECHNOLOGY

DEVELOPMENT

INCORPORATED

LIFE SCIENCES DIVISION

OCULAR EFFECTS OF NEAR INFRARED LASER RADIATION FOR SAFETY CRITERIA

JUNE, 1972

FINAL REPORT

Air Force Contract F41609-71-C-0016

Project 6301, Task 05, Work Unit 022

[illegible] School of Aerospace Medicine
Aerospace Medical [illegible]
[illegible] Air Force [illegible], Texas

8531 N. NEW BRAUNFELS AVE. • SAN ANTONIO, TEXAS 78217

UNCLASSIFIED
Security Classification

DOCUMENT CONTROL DATA - R&D
(Security classification of title, body of abstract and indexing annotation must be entered when the overall report is classified)

1. ORIGINATING ACTIVITY *(Corporate author)*
Technology Incorporated, Life Sciences Division
8531 N. New Braunfels Ave
San Antonio, Tx 78217

2a. REPORT SECURITY CLASSIFICATION
UNCLASSIFIED

2b. GROUP

3. REPORT TITLE
Ocular Effects of Near Infrared Laser Radiation for Safety Criteria

4. DESCRIPTIVE NOTES *(Type of report and inclusive dates)*
Final Report - March 1971 - June 1972

5. AUTHOR(S) *(Last name, first name, initial)*
Skeen, C.H.; Bruce, W. Robert; Tips, J.H., Jr.; Smith, M. Gearity; Garza, G.G.

6. REPORT DATE	7a. TOTAL NO. OF PAGES	7b. NO. OF REFS
June 1972	82	

8a. CONTRACT OR GRANT NO.	9a. ORIGINATOR'S REPORT NUMBER(S)
F41609-71-C-0016 b. PROJECT NO. c. 6301, Task 05 Work Unit 022 d.	9b. OTHER REPORT NO(S) *(Any other numbers that may be assigned this report)*

10. AVAILABILITY/LIMITATION NOTICES

Distribution of this document is unlimited

.1 .01 .05

11. SUPPLEMENTARY NOTES	12. SPONSORING MILITARY ACTIVITY
C	USAF School of Aerospace Medicine, Aerospace Medical Division (AFSC) Brooks Air Force Base, Texas 78235

13. ABSTRACT

Ocular effects of near infrared laser radiation were studied using a Nd^{3+} - YAG laser which emitted light at a wavelength of 1060 nm in the TEM_{00} mode. Retinal burn data were obtained on rhesus monkey eyes with the exposure duration used as a parameter. The exposures were for 1 sec, 10^{-1} sec, 10^{-2} sec, 10^{-3} sec and 7×10^{-7} sec durations and for trains of the 7×10^{-7} sec pulses with a pulse repetition rate of 1kHz lasting for 0.5 sec. Thirty eyes were irradiated for each exposure duration. The data were analyzed to find the energy per pulse corresponding to the retinal burn probability P=0.5 using (1) a probit analysis and (2) a straightforward arithmetical averaging of the retinal burn thresholds obtained for each eye. The values of the energy per pulse corresponding to the retinal burn probability P=0.5 were (43±2)mJ, (6.7±0.3)mJ, (1.4±0.1)mJ, (0.44±0.02)mJ, (24±1)μJ and (1.50±0.03)μJ, respectively, using the probit technique and (46±4)mJ, (6.9±0.6)mJ, (1.7±0.8)mJ, (0.454±0.005)mJ, (25±2)μJ, and (1.54±0.06)μJ, respectively, using the arithmetical averaging technique with confidence limit intervals of 95%. As required in this study, the 1 hour criterion for the appearance of ophthalmoscopically visible lesions was used. A major conclusion was that a cumulative effect exists for pulses in a repetitive pulse train, i.e., subthreshold pulses work in concert, in the pulse trains, to produce retinal lesions.

DD FORM 1 JAN 64 1473

ii
ii a

UNCLASSIFIED
Security Classification

UNCLASSIFIED
Security Classification

14. KEY WORDS	LINK A		LINK B		LINK C	
	ROLE	WT	ROLE	WT	ROLE	WT
Nd^{3+} - YAG laser; thermal injury; retinal burns; rhesus monkey; laser safeguards; laser safety standards						

INSTRUCTIONS

1. ORIGINATING ACTIVITY: Enter the name and address of the contractor, subcontractor, grantee, Department of Defense activity or other organization *(corporate author)* issuing the report.

2a. REPORT SECURITY CLASSIFICATION: Enter the overall security classification of the report. Indicate whether "Restricted Data" is included. Marking is to be in accordance with appropriate security regulations.

2b. GROUP: Automatic downgrading is specified in DoD Directive 5200.10 and Armed Forces Industrial Manual. Enter the group number. Also, when applicable, show that optional markings have been used for Group 3 and Group 4 as authorized.

3. REPORT TITLE: Enter the complete report title in all capital letters. Titles in all cases should be unclassified. If a meaningful title cannot be selected without classification, show title classification in all capitals in parenthesis immediately following the title.

4. DESCRIPTIVE NOTES: If appropriate, enter the type of report, e.g., interim, progress, summary, annual, or final. Give the inclusive dates when a specific reporting period is covered.

5. AUTHOR(S): Enter the name(s) of author(s) as shown on or in the report. Enter last name, first name, middle initial. If military, show rank and branch of service. The name of the principal author is an absolute minimum requirement.

6. REPORT DATE: Enter the date of the report as day, month, year; or month, year. If more than one date appears on the report, use date of publication.

7a. TOTAL NUMBER OF PAGES: The total page count should follow normal pagination procedures, i.e., enter the number of pages containing information.

7b. NUMBER OF REFERENCES: Enter the total number of references cited in the report.

8a. CONTRACT OR GRANT NUMBER: If appropriate, enter the applicable number of the contract or grant under which the report was written.

8b, 8c, & 8d. PROJECT NUMBER: Enter the appropriate military department identification, such as project number, subproject number, system numbers, task number, etc.

9a. ORIGINATOR'S REPORT NUMBER(S): Enter the official report number by which the document will be identified and controlled by the originating activity. This number must be unique to this report.

9b. OTHER REPORT NUMBER(S): If the report has been assigned any other report numbers *(either by the originator or by the sponsor)*, also enter this number(s).

10. AVAILABILITY/LIMITATION NOTICES: Enter any limitations on further dissemination of the report, other than those imposed by security classification, using standard statements such as:

(1) "Qualified requesters may obtain copies of this report from DDC."

(2) "Foreign announcement and dissemination of this report by DDC is not authorized."

(3) "U. S. Government agencies may obtain copies of this report directly from DDC. Other qualified DDC users shall request through _____."

(4) "U. S. military agencies may obtain copies of this report directly from DDC. Other qualified users shall request through _____."

(5) "All distribution of this report is controlled. Qualified DDC users shall request through _____."

If the report has been furnished to the Office of Technical Services, Department of Commerce, for sale to the public, indicate this fact and enter the price, if known.

11. SUPPLEMENTARY NOTES: Use for additional explanatory notes.

12. SPONSORING MILITARY ACTIVITY: Enter the name of the departmental project office or laboratory sponsoring *(paying for)* the research and development. Include address.

13. ABSTRACT: Enter an abstract giving a brief and factual summary of the document indicative of the report, even though it may also appear elsewhere in the body of the technical report. If additional space is required, a continuation sheet shall be attached.

It is highly desirable that the abstract of classified reports be unclassified. Each paragraph of the abstract shall end with an indication of the military security classification of the information in the paragraph, represented as *(TS)*, *(S)*, *(C)*, or *(U)*.

There is no limitation on the length of the abstract. However, the suggested length is from 150 to 225 words.

14. KEY WORDS: Key words are technically meaningful terms or short phrases that characterize a report and may be used as index entries for cataloging the report. Key words must be selected so that no security classification is required. Identifiers, such as equipment model designation, trade name, military project code name, geographic location, may be used as key words but will be followed by an indication of technical context. The assignment of links, rules, and weights is optional.

OCULAR EFFECTS OF NEAR INFRARED LASER RADIATION FOR SAFETY CRITERIA

FINAL REPORT

JUNE 1972

C. H. Skeen, Ph.D., W. Robert Bruce
J. H. Tips, Jr., M.S., M. Gearity Smith, B.S., G. G. Garza

Air Force Contract F41609-71-C-0016

Project 6301, Task 05, Work Unit 022

APPROVED BY:

James V. Benedict, Ph.D.
Manager, San Antonio Branch
Life Sciences Division

FOREWORD

The cooperation of the Vivarium personnel at Brooks Air Force Base, notably Sgts. E. L. Hendrix, F. W. Smith and A. E. Wiedeman, was outstanding and greatly appreciated. Special thanks are extended to Dr. Robert W. Ebbers for his assistance as the contract monitor, to Dr. Ebbers, Dr. Irving L. Dunsky and Mr. E. O. Richey for many helpful consultations throughout this study and to Mr. Richard McNee for calling to our attention a possible fundamental difficulty in applying the probit analysis to retinal burn data.

The work in the animal holding facilities and in the animal preparations at Technology Incorporated done by Mr. Robert Neish and Mr. Peter Herrera, and the photographic service supplied by Mr. Richard Johnson was most helpful as was the art work done by Mr. Hector Lizcano.

Special thanks are accorded to Dr. Ralph G. Allen, Dr. J. V. Benedict and Dr. Martin M. Mainster for numerous conferences which helped immensely in our understanding and in our interpretation of our experimental results.

Finally, our appreciation is hereby expressed to Mrs. Linda Anderson for typing this draft final report and for her secretarial support throughout this program.

LIST OF FIGURES

LIST OF TABLES

TABLE OF CONTENTS

1. INTRODUCTION

The light emitted by lasers is highly collimated, nearly monochromatic and very intense. Because of its good collimation and high intensity, laser light is potentially hazardous to both the human skin and the human eye.

The eye is quite vulnerable to the laser light (visible and near infrared wavelengths) which is transmitted efficiently by the intraocular media. This vulnerability arises because the transmitted light is focussed into a small spot on the retina by the optics of the eye. The fluence (energy per unit area) incident on the cornea can be quite small and still be very hazardous because the fluence at the retina is amplified by a factor of about 10^5 relative to the fluence at the cornea.

Since it is a requirement that lasers be operated safely, many experiments are performed to determine the extent of the vulnerability of the eye to the laser light which it transmits efficiently. These experiments are designed to find the extent of this vulnerability by the determination of the retinal burn threshold for the eye when the cornea is irradiated by laser light at a given wavelength, a given beam divergence and for a given exposure level and duration. These retinal burn thresholds are used to establish permissible exposure levels (PEL). The PEL are considered as safe exposure levels for personnel working either with or in the vicinity of the corresponding laser systems. Safeguard procedures can be instituted to ensure that

personnel do not receive ocular exposures from a laser in excess of the PEL.

In the retinal burn experiments, eyes are irradiated with laser light and the retinas are observed ophthalmoscopically following an exposure. Although the duration of the observation times used by some workers in the past were as short as about 5 min and as long as about 24 hours, the observation time generally used now is 1 hour. Most experiments are currently being performed on the Macaca Mulatta (rhesus monkey) with the results extrapolated to humans by using an arbitrary variability factor between the species.

Some early work was performed[1] to determine retinal burn thresholds for rhesus monkeys exposed to the 1060 nm light from a Nd^{3+}-YAG laser where the one-hour criterion for the observation of ophthalmoscopically visible lesions was used. The laser used in this early work was operated in both the cw and in the Q-switched mode. The cw radiation was pulsed using an electronically controlled camera shutter to obtain pulses with durations (full-width-at-half-maximum-power, FWHMP) of 10^{-2} sec, 10^{-1} sec and 1 sec. The Nd^{3+}-YAG laser used for this study was Q-switched using a rotating mirror-prism to obtain pulses with 30 nsec FWHMP. The retinal burn thresholds were found to depend upon the duration of the exposures, with the energy per pulse being smaller for the shorter exposure times,

It is believed that the retinal damage from the laser radiation in these experiments[1] and in other experiments[2-4] is produced thermally. This corresponds to the irradiated and contiguous chorioretinal tissues being raised to a critical temperature for a given time and a lesion being produced. Clearly, to first order approximations, there should be an irradiated spot-size-effect, i.e., the smaller the retinal spot irradiated, the smaller the amount of energy required to cause the heated tissues to reach the critical temperature. This spot-size-effect was demonstrated first experimentally using a white light source[5] and later using a laser light[6] source.

For lasers, the retinal spot size depends upon the laser beam divergence and the refracting properties of the eye; and, the diameter is estimated by the product of the divergence (full angle) and the focal length of the eye. The divergence is related to the energy distribution in the laser beam wavefront. This energy distribution is described in terms of modes[7] using the symbol TEM_{ij}. The i and j subscripts refer to the nodes in the transverse electromagnetic field in the laser cavity. The mode having the lowest order is the TEM_{00} one. The energy distribution in the wavefront for the TEM_{00} mode is Gaussian. This TEM_{00} energy distribution is diffraction limited and; consequently, it is the smallest beam divergence possible without using ancillary optics. Hence a laser with its output in the TEM_{00} mode will have a smaller retinal spot size than any other radiation mode from this laser.

It is neither feasible economically nor feasible from a point-of-view of the time necessary to perform experiments to determine PEL for every conceivable laser operating case. To keep from performing this very large number of measurements, sets of credible "worst-case" experiments are performed. In these credible "worst case" experiments the smallest retinal spot size is obtained by using TEM_{00} mode laser light and by using essentially emmetropic eyes (eyes that are corrected for refractive errors and chromatic aberrations using ophthalmic lenses and relaxed by sedation).

Since no previous "worst case" experiments were performed using 1060nm laser radiation, work was performed using a Nd^{3+}-YAG laser operating at a wavelength of 1060nm in the TEM_{00} mode. The results of this effort are reported in this document. The laser used in this work was pulsed to give exposures with FWHMP of 1 sec, 10^{-1} sec, 10^{-2} sec, 10^{-3} sec and 7×10^{-7} sec. Moreover, no previous work was performed to study systematically the ocular effects of repetitive pulse lasers. Since repetitive pulse lasers are being used and since it is a requirement that they be operated safely, some preliminary work was performed in this study using the Nd^{3+}-YAG system. The Nd^{3+}-YAG laser was pulsed to give a pulse train of the 7×10^{-7} sec pulses at a pulse repetition rate of 1kHz and lasting for 0.5 sec. The results of this preliminary repetitive pulse work are reported also in this document.

2. EXPERIMENTAL PROCEDURES

2.1 Laser System

The laser used in the experiments, described in this report, was a Coherent Radiation, Inc. model 60 YAG system (see Appendix A for the details of mode control, etc.). A photograph of this system with a cover removed is shown in Figure 1. This system was operated in the cw time regime, the Q-switched time regime and the repetitive pulse time regime. It emitted laser radiation at a wavelength of 1060nm in the TEM_{00} mode. The diameter of the limiting aperture in the laser cavity was 2.0mm and the corresponding beam divergence (full angle) was about 1.2 milliradians. The laser light was circularly polarized.

The peak power emitted during the cw portion of the experiments was 2.4 watts in the TEM_{00} mode. The peak power emitted in a single 7×10^{-7} sec pulse was 2 kw. The peak power per pulse for the repetitive pulse time regime operation was 0.5 kw using the pulse repetition rate of 1 kHz.

2.2 Exposure Durations and Laser Calibrations

An electronically controlled camera-shutter was used to obtain exposure durations of 1 sec. An electronically controlled camera-shutter synchronized with a rotating-slotted-wheel was used to obtain

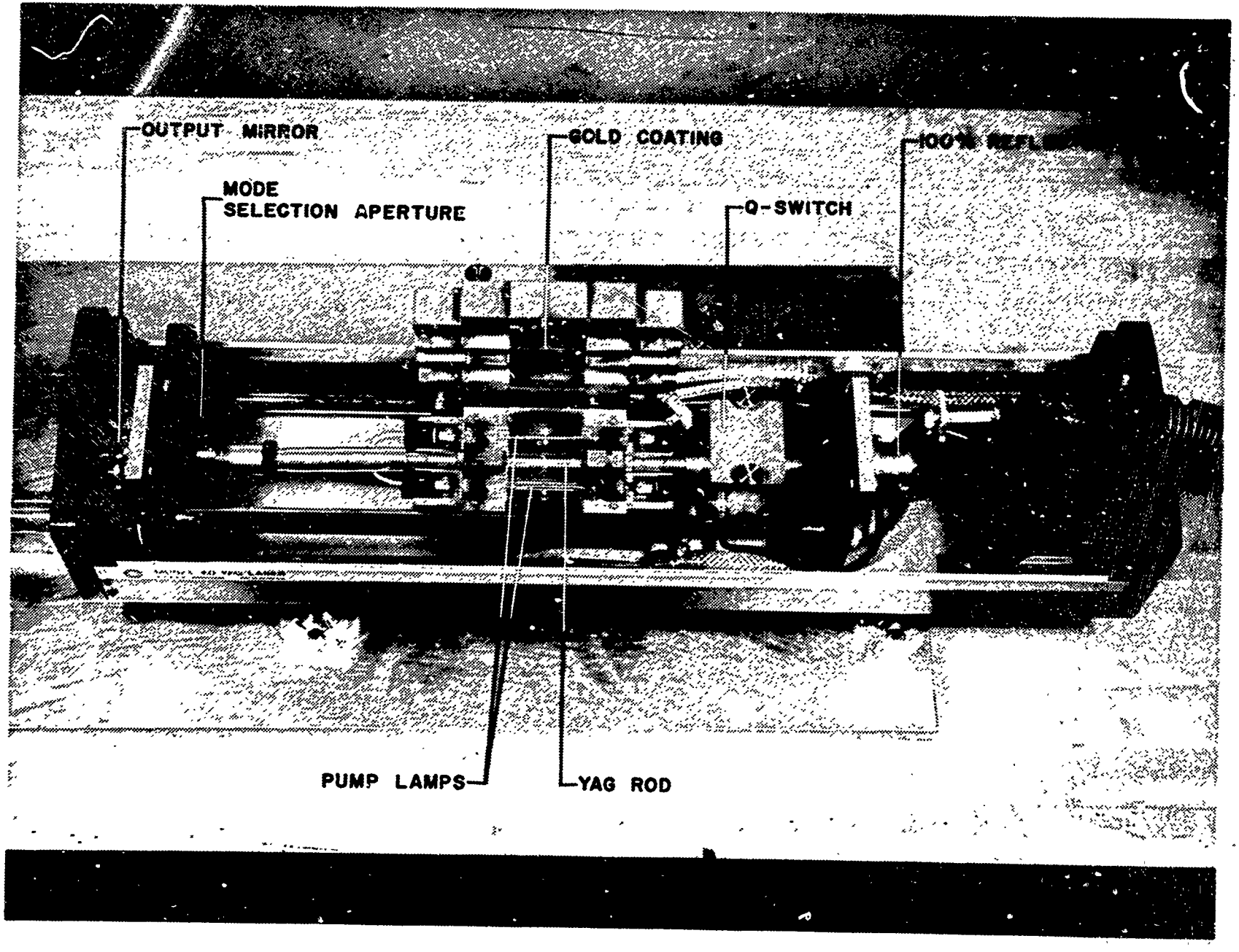

Figure 1 The YAG Laser with the Top Cover Removed to Show Key Components

the 10^{-1} sec, 10^{-2} sec and 10^{-3} sec duration exposures. The Coherent Radiation, Inc. model 460 Acoustic Q-switch was used to obtain the 7×10^{-7} sec duration exposures. A Q-switch controller-box was operated either manually or by external triggering to obtain the single Q-switched pulses. The Q-switch controller-box was operated either internally or triggered externally with an appropriate electronic pulse and waveform generator to obtain the trains of 7×10^{-7} sec pulses. The details of the techniques used to obtain the exposure durations are outlined in Appendix B..

The temporal variation of the laser power in a pulse emitted by the laser as configured for these experiments was detected with an EG&G silicon photodiode, model SGD-100, in conjunction with a Tektronix model 555 dual beam oscilloscope. The laser output power as detected by this oscilloscope-diode array was calibrated using two devices with calibrations traceable to NBS values. One of the devices was a HADRON/TRG model 100 ballistic thermopile and the other one was a Coherent Radiation, Inc. model 201 power meter. The waveforms were recorded and the energy per pulse was measured for every ocular irradiation performed during this study. The details of the calibration procedures are discussed in Appendix B.

2.3 Primate Housing and Primate Preparations

The animal housing facility at the Life Sciences Division of Technology Incorporated has a carefully controlled environment where the primates

are individually housed in modern stainless steel cages. The animals and facility are maintained in accordance with the "Guide for Laboratory Animals, Facilities and Care" as published by the National Academy of Sciences - National Research Council. Regular inspections were made by a representative of the U. S. Department of Agriculture, Agricultural Research Service, Animal Health Division.

Primate preparation for various experimental procedures were carried out in the animal surgery suite. The surgery suite consisted of a preparation room, a scrub room, and an operating room. Initial preparations (e.g., sedation, pupil dilation, body weight determination) were performed in the surgery preparation room. The operating room was modern and equipped for the most sophisticated experimental preparations and procedures.

On the day prior to the retinal irradiations of a primate, atropine sulfate, 1% ophthalmic ointment was introduced into the conjunctival sac. This procedure was utilized to give maximum pupillary dilation. Just prior to the retinal irradiations, the primate was tranquilized with phencyclidine hydrochloride (Sernylan) 20mg/cc, IM. The dosage employed was 1 mg/Kg of body weight. Then an anesthetizing procedure was started by introducing a 19 gauge intraveneous catheter into a posterior superficial vein in a leg. Intitally 0.5 cc of sodium pentobarbital, (Nembutal) 50 mg/cc, was administered by way of the intracatheter, and

smaller increments were injected as necessary to maintain deep anesthesia. Lacrimation was usually suppressed by anesthesia; therefore, the eye was frequently irrigated with normal saline or artificial tears to preserve corneal transparency.

Following anesthetization, thorough opthalmoscopic and slit-lamp examinations of the eyes were performed. Following the slit-lamp examination, the refractive error for each eye of the primate was determined with a retinoscope. Refractive errors for chromatic aberration were determined with a retinoscope in conjunction with band-pass filters at 475, 517, and 610nm. The corrective lens necessary at a wavelength of 475nm was -0.5 diopter, at 517nm it was -0.25 diopter and at 610nm it was +0.25 diopter. Based on these results, it was estimated that the corrective lens for chromatic aberration at 1060nm was +0.5 diopter[8][9]. The necessary corrective lens was used for each rhesus monkey eye irradiated.

Finally; during the irradiations, a 402 rectal probe and Yellow Springs model 72 Tele-Thermometer were used at all times to monitor primate core temperature.

2.4 Retinal Irradiations

Key components of the Nd^{3+}-YAG laser system and key components of the laser energy delivery system for placement of radiation in an

eye during these experiments are shown in the photograph in Figure 2. The details of the operation of this equipment for this study are given in Appendices A and B.

A sequence of events during a retinal irradiation procedure was as follows. The cornea of an eye of an anesthetized primate was cleared and a site in the macular area selected. The cross-hairs of an ophthalmoscope light were positioned so as to intersect at the chosen site. A solenoid on the ophthalmoscope was energized and the "pop-up" mirror came into place. An electronic signal in the form of a voltage pulse was received then by either the camera-shutter, or by the camera shutter and rotating-wheel combination or by the Q-switch controller-box. This procedure permitted one and only one pulse or pulse train to be emitted by the laser and focussed onto the retina with the eye's own optics together with any required lens correction.

"Marker burns", which served as fiducial points, were placed at the corners of a square with 1.5mm diagonal centered on the fovea. Up to 26 independent irradiations including the "marker burns" were placed in the macular region. All exposures, with the exception of the "marker burns" were placed at random in the macula.

A fundus photograph, of a rhesus monkey eye, like those taken routinely during this study is shown in Figure 3. A schematic diagram of the

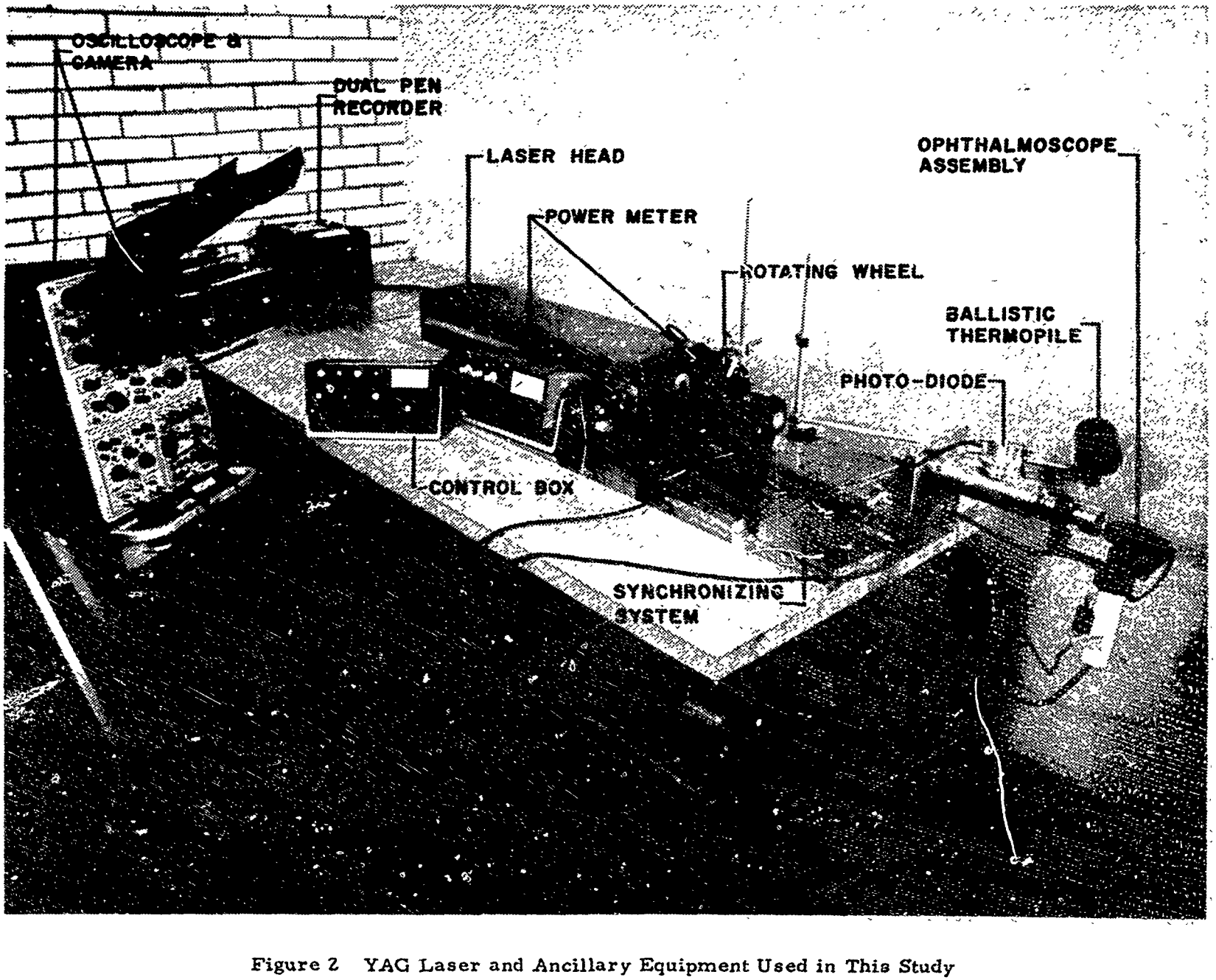

Figure 2 YAG Laser and Ancillary Equipment Used in This Study

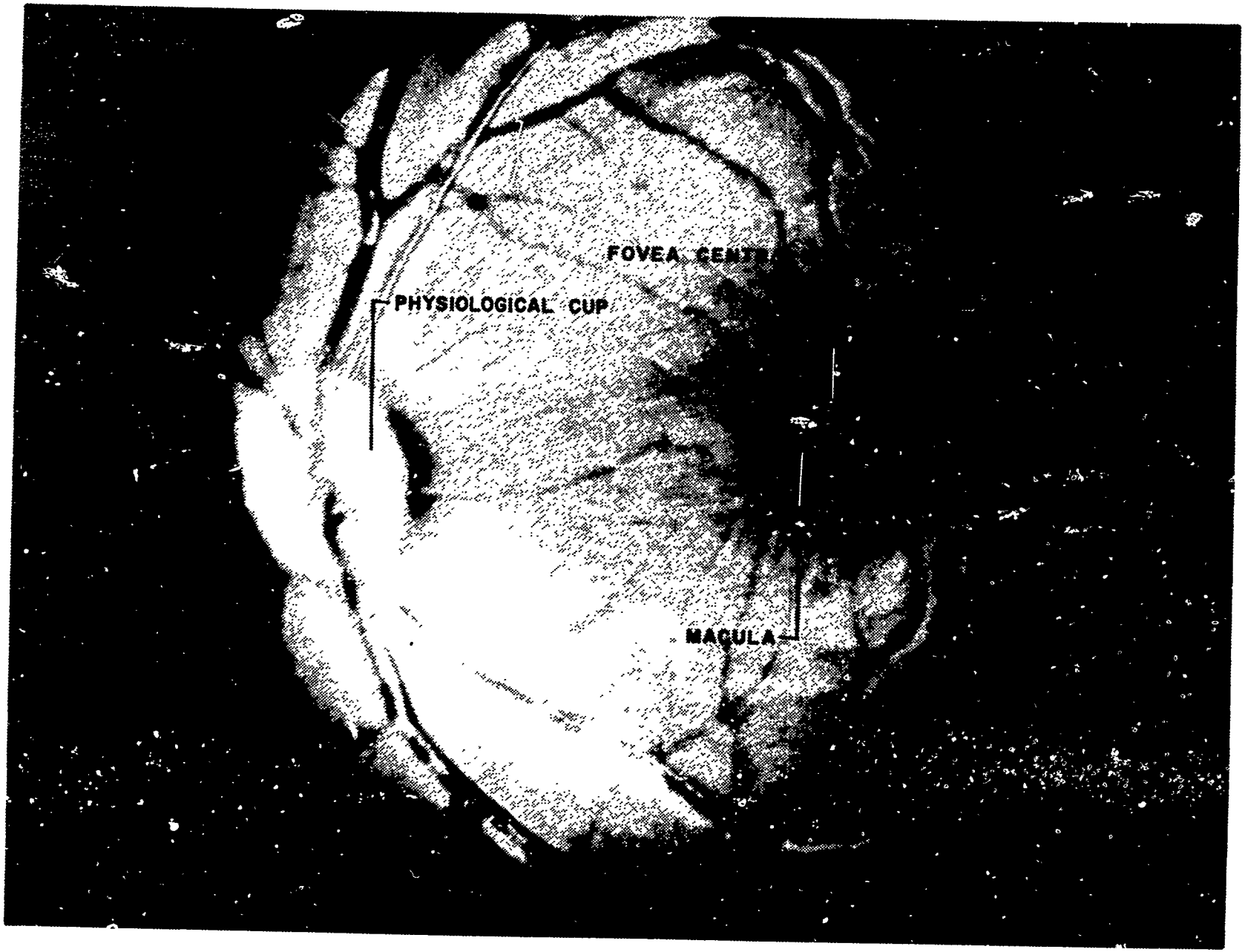

Figure 3 Typical Fundus of a Macaca Mulatta (rhesus monkey)

macular region typical of a rhesus monkey fundus is shown in Figure 4. A pattern of the irradiation sites used is shown in Figure 5. This irradiation pattern was varied for each eye irradiated. The power of the laser light at the cornea was varied in turn for the different retinal irradiations. The irradiated sites were observed periodically at time intervals up to an hour subsequent to the irradiations and a record made as to whether or not a lesion appeared. From these data, a retinal burn threshold was determined for each eye.

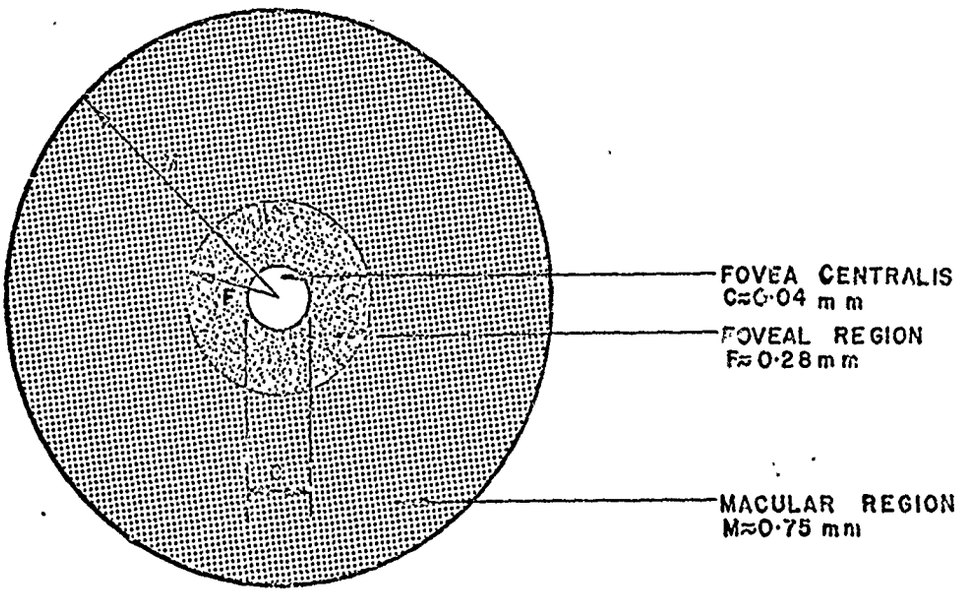

Figure 4. Schematic Diagram of the Macular Region of the Macaca Mulatta (rhesus monkey) Fundus

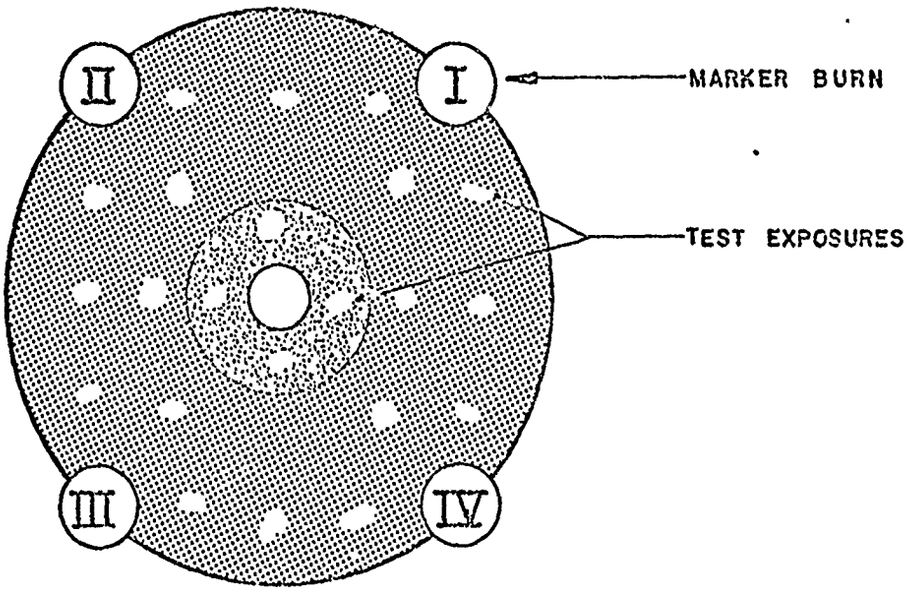

Figure 5. Diagram Showing "Marker Burn" Locations and Typical Irradiation Pattern

3. EXPERIMENTAL RESULTS

3.1 Variable Duration cw Experiments

Waveforms typical of those recorded for the 1 sec, 10^{-1} sec, 10^{-2} sec and 10^{-3} sec FWHMP pulses chopped from the cw laser radiation are shown at A, B, C and D, respectively, in Figure 6. These are tracings of the actual waveforms that were recorded on polaroid film for a permanent record.

Data like those from which the retinal burn thresholds were determined are shown in Tables I through IV for the 1 sec, 10^{-1} sec, 10^{-2} sec and 10^{-3} exposures, respectively. The corresponding retinal burn thresholds obtained from an analysis of the data secured are summarized in Tables V through VIII.

Data like those listed in Tables I through IV were analyzed using a probit technique[10] (see Appendix C for details of the probit analysis used in this study). The results of the probit analysis are shown in Figures 7 through 10 for the 1 sec, 10^{-1} sec, 10^{-2} sec and the 10^{-3} sec duration exposures, respectively. In each of the Figures 7-10, the retinal burn probability is plotted versus the energy per pulse incident on the cornea.

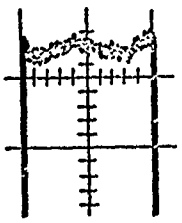

0.5 v/cm, 0.5 sec/cm

A.

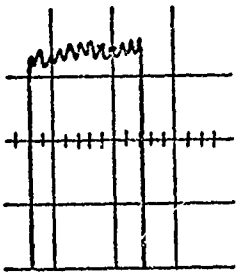

0.2 v/cm, 0.05 sec/cm

B.

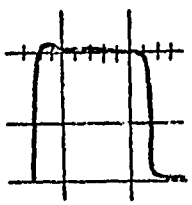

0.5 v/cm, 5 msec/cm

C.

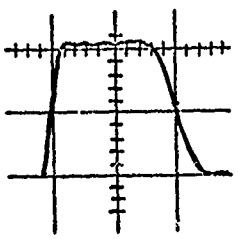

0.2 v/cm, 0.5 msec/cm

D.

Figure 6. Waveforms Typical of those used in the Pulsed cw Experiments. A, B, C, and D Represent Waveforms for 1 sec, 10^{-1} sec, 10^{-2}, and 10^{-3} sec, Respectively.

TABLE I. Retinal Burn Threshold Data for 1 sec Duration Pulses of 1060nm. Laser Light (Eye No. 15).

IRRADIATION NUMBER	ENERGY PER PULSE mJ	BURN/NO BURN 1 HR. CRITERION
1	124	Burn
2	124	Burn
3	115	Burn
4	110	Burn
5	110	Burn
6	90	Burn
7	83	Burn
8	76	Burn
9	70	Burn
10	62	Burn
11	55	Burn
12	52	No Burn
13	48	No Burn
14	44	No Burn
15	41	No Burn
16	39	No Burn
17	34	No Burn
18	28	No Burn
19	21	No Burn

TABLE II. Retinal Burn Treshold Data for 10^{-1} sec Duration Pulses of 1060nm Laser Light (Eye No. 44).

IRRADIATION NUMBER	ENERGY PER PULSE mJ	BURN/NO BURN 1 HR. CRITERION
1	.13	Burn
2	12	Burn
3	12	Burn
4	11	Burn
5	11	Burn
6	10	Burn
7	9.6	Burn
8	9.0	Burn
9	8.4	Burn
10	7.8	No Burn
11	7.2	No Burn
12	6.0	No Burn
13	5.4	No Burn
14	4.9	No Burn
15	4.2	No Burn
16	3.6	No Burn

TABLE III. Data for Retinal Burn Threshold for 10^{-2} sec Duration Pulses of 1060nm Laser Light (Eye No. 79).

IRRADIATION NUMBER	ENERGY PER PULSE mJ	BURN/NO BURN 1 HR. CRITERION
1	2.8	Burn
2	2.7	Burn
3	2.4	Burn
4	2.2	Burn
5	1.9	Burn
6	1.7	Burn
7	1.6	Burn
8	1.6	Burn
9	1.5	No Burn
10	1.4	No Burn
11	1.4	No Burn
12	1.2	No Burn
13	1.1	No Burn
14	.9	No Burn
15	.8	No Burn
16	.7	No Burn

TABLE IV. Retinal Burn Threshold Data for 10^{-3} sec Duration Pulses of 1060nm Laser Light (Eye No. 110).

IRRADIATION NUMBER	ENERGY PER PULSE mJ	BURN/NO BURN 1 HR. CRITERION
1	2.1	Burn
2	1.7	Burn
3	.75	Burn
4	.66	Burn
5	.59	Burn
6	.55	Burn
7	.52	Burn
8	.48	Burn
9	.46	No Burn
10	.43	No Burn
11	.37	No Burn
12	.34	No Burn
13	.28	No Burn
14	.25	No Burn
15	.21	No Burn
16	.17	No Burn

Table V. Retinal Burn Thresholds for 1 sec Duration Exposures.

Eye	Threshold mJ
1	45.7
2	42.0
3	67.7
4	47.5
5	60.2
6	47.9
7	40.2
8	46.6
9	47.6
10	33.4
11	34.4
12	45.4
13	43.8
14	47.5
15	53.8
16	78.7
17	44.0
18	52.4
19	38.9
20	66.7
21	65.6
22	42.9
23	33.3
24	35.6
25	28.7
26	45.8
27	49.0
28	36.9
29	31.3
30	41.5
31	40.4
32	33.3

Table VI. Retinal Burn Thresholds for 10^{-1} sec Duration Exposures.

Eye	Threshold mJ
33	7.44
34	10.40
35	10.34
36	6.42
37	7.77
38	5.24
39	5.94
40	7.47
41	8.08
42	7.47
43	6.14
44	8.08
45	5.67
46	8.07
47	9.42
48	8.07
49	6.70
50	6.14
51	6.14
52	6.49
53	6.48
54	7.07
55	6.49
56	5.74
57	6.32
58	6.31
59	5.17
60	4.02
61	4.60
62	6.57
63	7.17

Table VII. Retinal Burn Thresholds for 10^{-2} sec Duration Exposures.

Eye	Threshold mJ
64	1.58
65	1.50
66	1.45
67	1.52
68	1.45
69	1.38
70	1.45
71	1.51
72	1.45
73	1.52
74	1.39
75	4.73
76	4.38
77	1.59
78	1.62
79	1.55
80	1.42
81	1.39
82	1.51
83	1.52
84	1.66
85	1.28
86	0.88
87	1.69
88	1.54
89	1.52
90	1.59
91	1.52
92	1.73
93	1.65

Table VIII. Retinal Burn Thresholds for 10^{-3} sec. Duration Exposures.

Eye	Threshold μJ
94	525
95	576
96	440
97	508
98	440
99	423
100	669
101	508
102	457
103	423
104	457
105	449
106	475
107	502
108	398
109	502
110	475
111	447
112	449
113	404
114	448
115	449
116	448
117	395
118	484
119	449
120	359
121	314
122	341
123	398

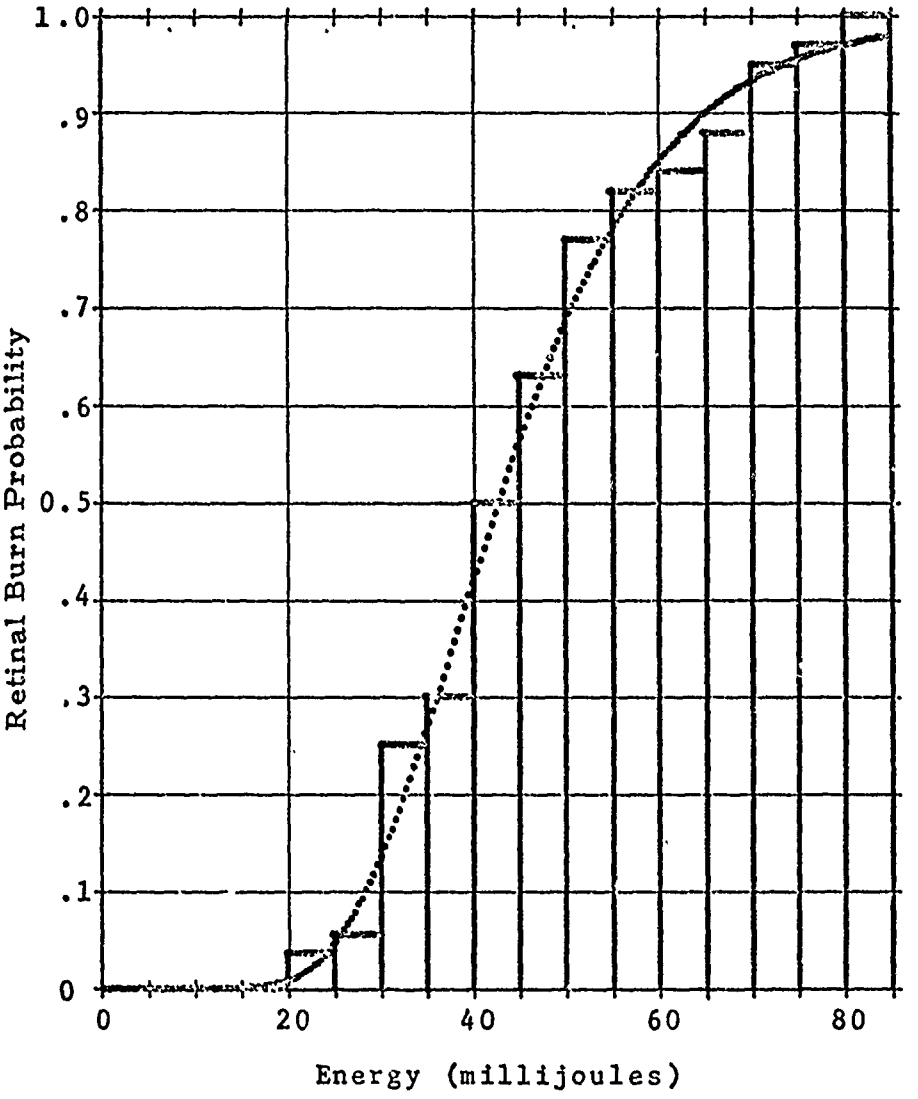

Fig. 7. Retinal Burn Probability versus the Energy Per 1 sec Duration Pulse of the 1060 nm Laser Light (30 Eyes).

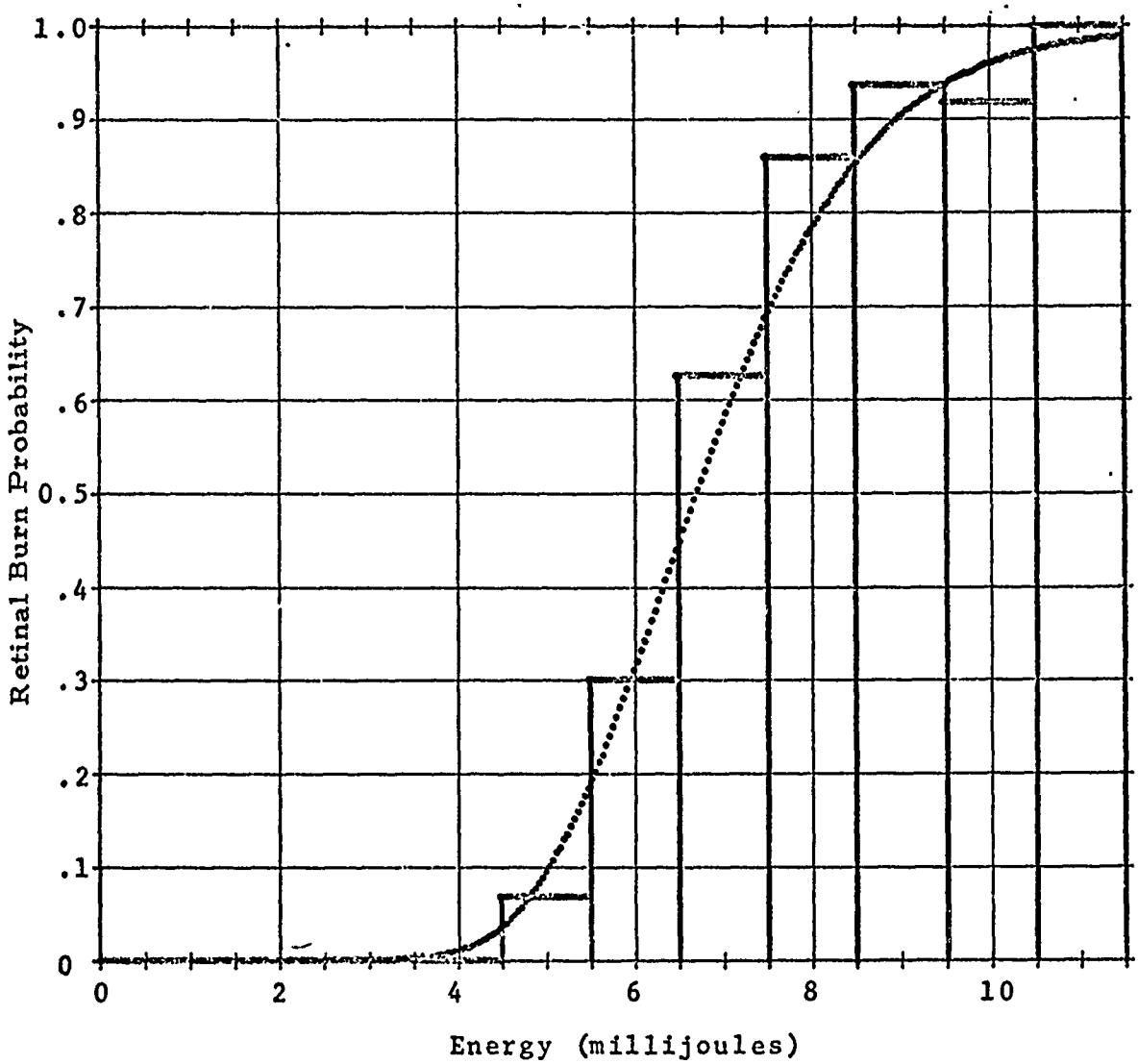

Fig. 8. The Retinal Burn Probability Versus Energy Per 10^{-1} sec Duration Pulse of 1060 nm Laser Light (30 Eyes).

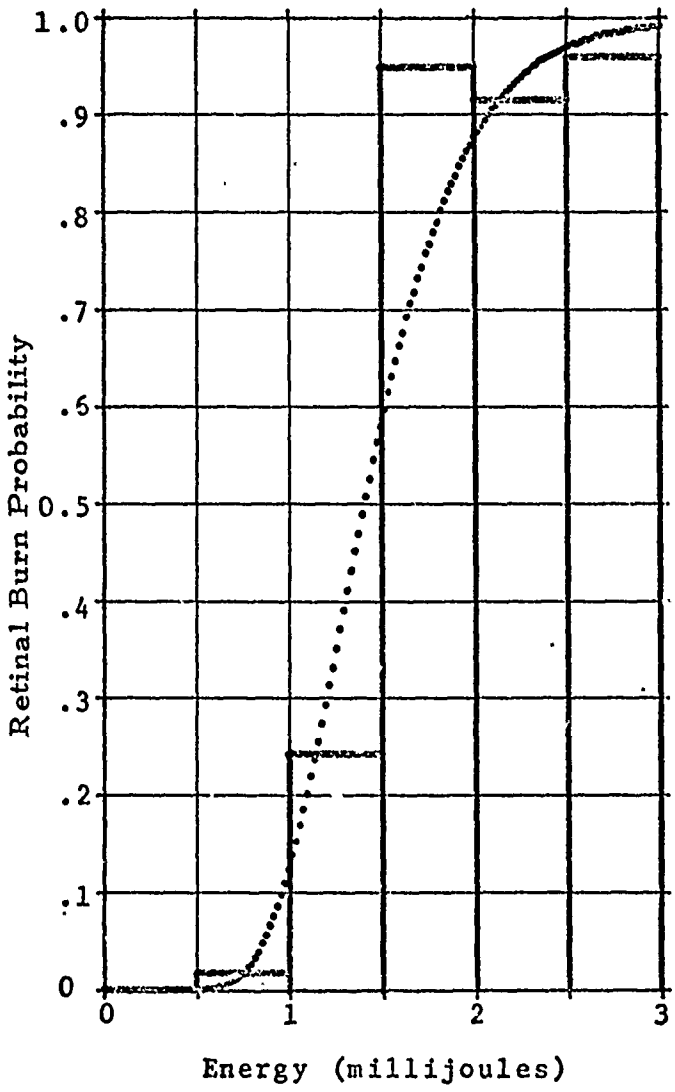

Fig. 9. Retinal Burn Probability as a Function of the Energy Per 10^{-2} sec Duration Pulse of the 1060 nm Laser Light (30 Eyes).

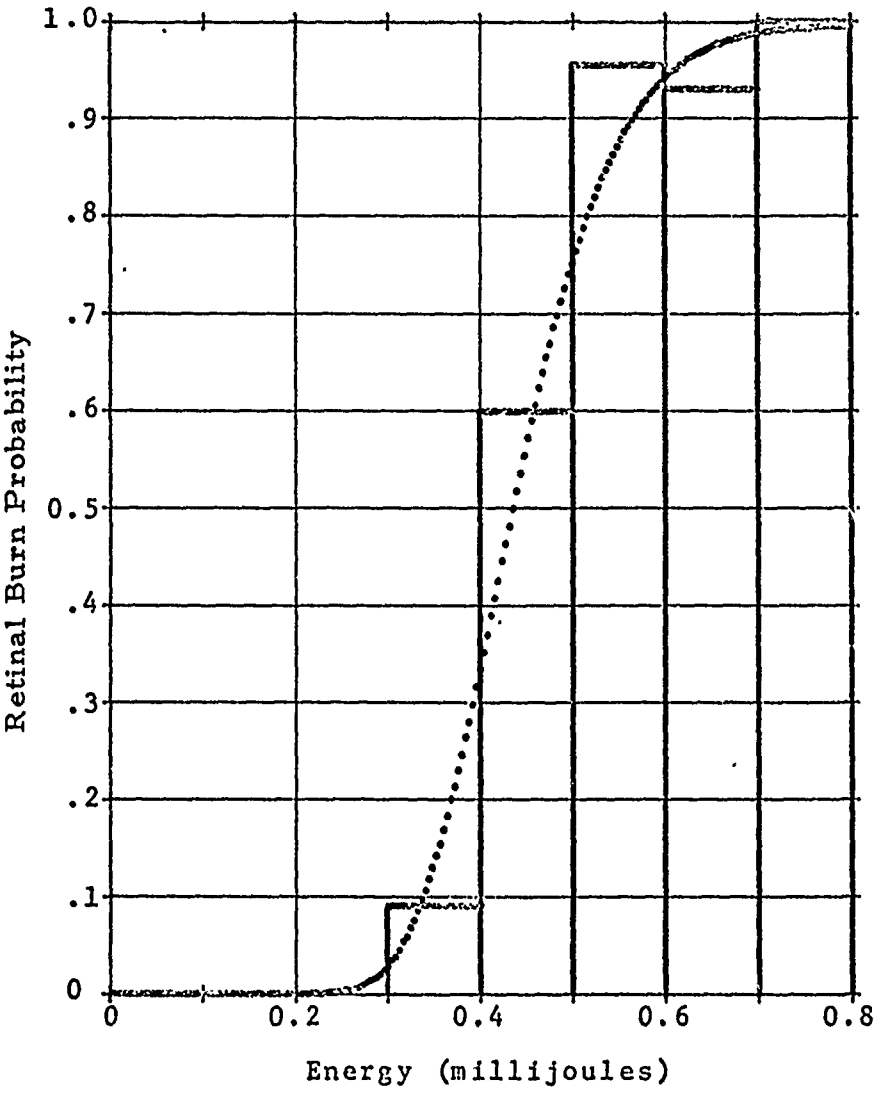

Fig. 10. Retinal Burn Probability versus the Energy Per 10^{-3} sec Duration Pulse of the 1060 nm Laser Light (30 Eyes).

3.2 Q-Switched Pulse Experiments

A waveform typical of those used during the Q-switched pulse exposures of the primate eyes is shown in Figure 11 which is a tracing from the permanent record on polaroid film. The FWHMP of the Q-switched pulses was 7×10^{-7} sec.

Data typical of those from which the retinal burn thresholds were determined are shown in Table IX. The corresponding retinal burn thresholds obtained from an analysis of these data are shown in Table X.

The data like those shown in Table IX, from 30 primate eyes, were analyzed using the probit technique. A portion of the results obtained from this probit analysis is shown graphically in Figure 12 where the retinal burn probability is plotted versus the energy per pulse at the corneas irradiated.

3.3 Q-Switched Pulse Train Experiments

Trains of the 7×10^{-7} sec pulses (like .at pulse shown in Figure 11) at a pulse repetition rate of 1 kHz and lasting for 0.5 sec were used to irradiate primate eyes. Retinal burn data typically obtained during these pulse train experiments are displayed in Table XI. The retinal burn thresholds obtained from the analysis of data like those in Table XI for 30 primate eyes are summarized in Table XII.

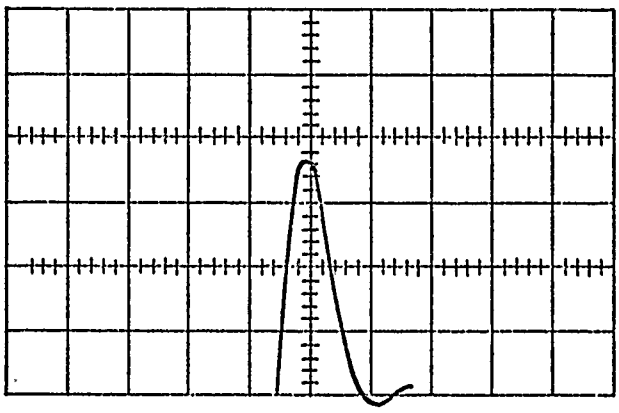

Figure 11. Tracing of a Typical Single 0.7 μ sec Pulse at a Wavelength of 1060 nm (Vertical Sensitivity of Oscilloscope was 20 v/cm and the Sweep Rate was 1 μsec/cm)

Table IX. A Sample of Retinal Burn Data for Single 0.7 μsec Exposures of a Rhesus Monkey Eye to the 1060 nm Laser Light. (Eye No. 146)

Exposure	Energy (μJ) for 0.7 μsec Pulses	Burn/No Burn 1 Hr. Criterion
1	105	Burn
2	90	Burn
3	75	Burn
4	60	Burn
5	45	Burn
6	30	Burn
7	26	Burn
8	24	Burn
9	22	No Burn
10	19	No Burn
11	17	No Burn
12	16	No Burn
13	13	No Burn
14	10	No Burn

Table X. Retinal Burn Thresholds for 7×10^{-7} sec Duration Exposures.

Eye	Threshold μJ
124	42.7
125	42.7
126	23.3
127	23.3
128	22.6
129	24.8
130	20.4
131	21.5
132	19.4
133	25.3
134	23.9
135	21.8
136	17.7
137	17.7
138	21.8
139	23.9
140	24.2
141	24.1
142	24.2
143	24.1
144	27.5
145	31.1
146	22.7
147	27.5
148	25.1
149	25.1
150	29.0
151	29.0
152	19.6
153	19.6

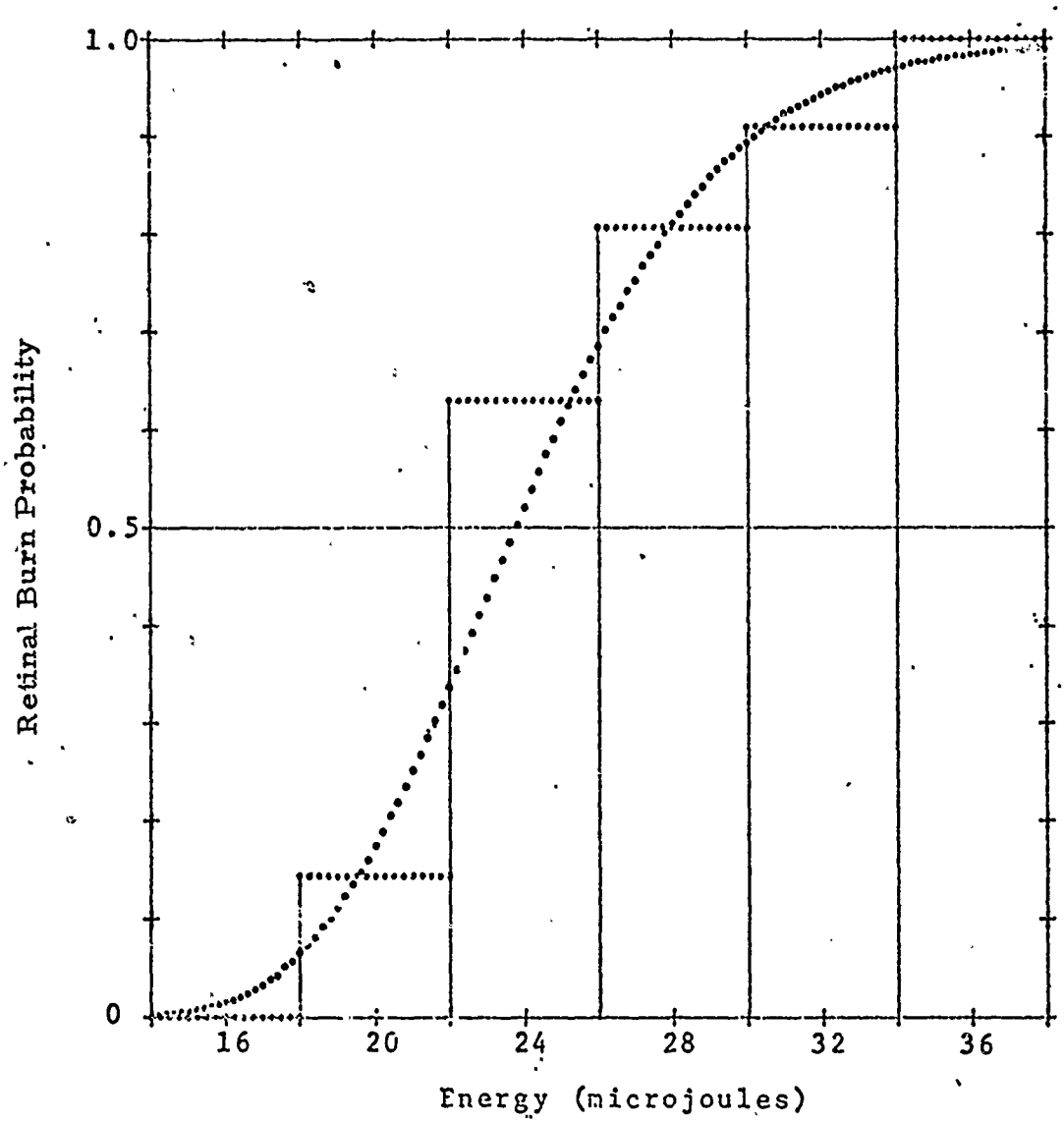

Figure 12. Retinal Burn Probability versus Energy of the Single 0.7μ sec Laser Pulses at a Wavelength of 1060 nm (30 Eyes).

Table XI. A Sample of Retinal Burn Data for a Train of 0.7 μsec Exposures of a Rhesus Monkey Eye to the 1060 nm Laser Light. (Eye No. 179)

Exposure	Energy μJ Per 0.7 μsec Pulse	Burn/No Burn 1 Hr. Criterion
1	10.8	Burn
2	8.0	Burn
3	7.0	Burn
4	6.5	Burn
5	2.0	Burn
6	1.9	Burn
7	1.7	Burn
8	1.6	Burn
9	1.5	Burn
10	1.45	Burn
11	1.3	No Burn
12	1.2	No Burn
13	1.1	No Burn
14	.96	No Burn
15	.83	No Burn

Table XII. Retinal Burn Threshold for Trains of 7×10^{-7} sec Pulses at Pulse Repetition Rate of 1 kHz Lasting for 0.5 sec.

Eye	Threshold (Energy per Pulse) μ J
154	2.03
155	1.48
156	1.41
157	1.33
158	1.76
159	1.62
160	1.61
161	1.75
162	1.61
163	1.61
164	1.52
165	1.81
166	1.52
167	1.67
168	1.46
169	1.46
170	1.32
171	1.46
172	1.78
173	1.50
174	1.78
175	1.39
176	1.50
177	1.50
178	1.39
179	1.38
180	1.38
181	1.38
182	1.38
183	1.39

A probit analysis was performed on the retinal burn data, like those shown in Table XI, for 30 primate eyes exposed in the Q-switched pulse train experiments. Some results obtained with this probit analysis are shown graphically in Figure 13 where the retinal burn probability is plotted versus the energy per pulse at the corneas during the pulse train exposures.

3.4 ED50 or P=0.5 Energy Values

Quantities of prime importance obtained from this study are the retinal burn thresholds for the Macaca Mulatta exposed to the 1060 nm light for a given time interval. The retinal burn threshold is by definition the energy per pulse which, when incident on the cornea, is expected to produce a retinal lesion (the 1hr criterion was required in this study) in 50% of the Macaca Mulatta having normal emmetropic eyes when this energy is focused into an exposed site in the macular region. These retinal burn thresholds are called the ED50 values or the retinal burn probabilities P=0.5. The ED50 or the P=0.5 energy values can be obtained from either a probit analysis or from the mean of the retinal burn thresholds for a set of primate eyes. The ED50 or P=0.5 values obtained from these analyses for this study are shown in Table XIII. These results and the other results described in this section will be discussed further in the following section of this report.

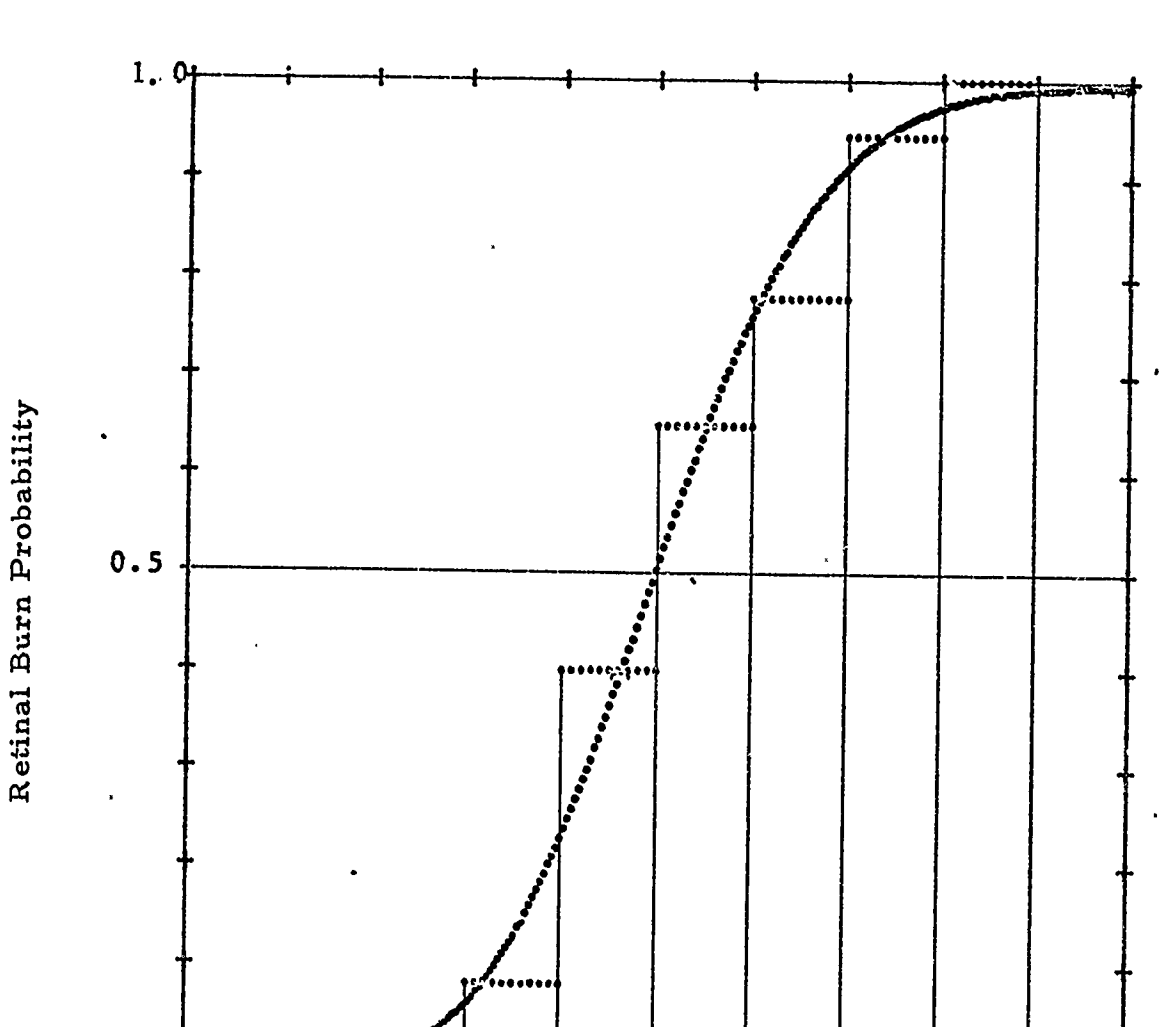

Figure 13. Retinal Burn Probability versus Energy per Pulse in the Train of 0.7 μsec Laser Pulses at a Wavelength of 1060 nm. (30 Eyes)

Table XIII. Energy Per Pulse Corresponding to the Retinal Burn Probability, P=0.5 or ED50 Values for Single Laser Pulse Durations from 7×10^{-7} sec to 1 sec and for a Repetitive Pulse Train.

PULSE DURATION sec	ENERGY/PULSE mJ Probit Analysis	ENERGY/PULSE mJ Average
7×10^{-7}	$(24 \pm 1) \times 10^{-3}$	$(25 \pm 2) \times 10^{-3}$
3.5×10^{-4} (effective exposure duration for the pulse train)	$(1.5 \pm 0.03) \times 10^{-3}$	$(1.54 \pm 0.06) \times 10^{-3}$
1×10^{-3}	0.44 ± 0.02	0.454 ± 0.005
1×10^{-2}	1.4 ± 0.1	1.7 ± 0.8
1×10^{-1}	6.7 ± 0.3	6.9 ± 0.6
1	43 ± 2	46 ± 4

4. DISCUSSION OF RESULTS

The retinal burn threshold energies obtained from the data analysis were converted to retinal burn threshold powers by using the ED50 values and the corresponding FWHMP. The results for conversion of the retinal burn threshold energy values to threshold power values are shown in Table XIV. These retinal burn thresholds, in terms of power, were plotted on a log-log scale versus the exposure duration for the single pulse irradiations and the effective exposure time (the product of the number of pulses in the train, and the FWHMP) for the pulse train irradiation of primate eyes. These results are shown graphically in Figure 17.

Table XIV Power Per Pulse Corresponding to the Retinal Burn Probability, P=0.5, for Laser Pulse Durations from 7×10^{-7} sec to 1 sec and for a Repetitive Pulse Train.

DURATION SEC	POWER/PULSE WATTS
7×10^{-7}	34.3
3.5×10^{-4} (effective exposure duration for the pulse train)	2.1
1×10^{-3}	0.440
1×10^{-2}	0.140
1×10^{-1}	0.067
1	0.043

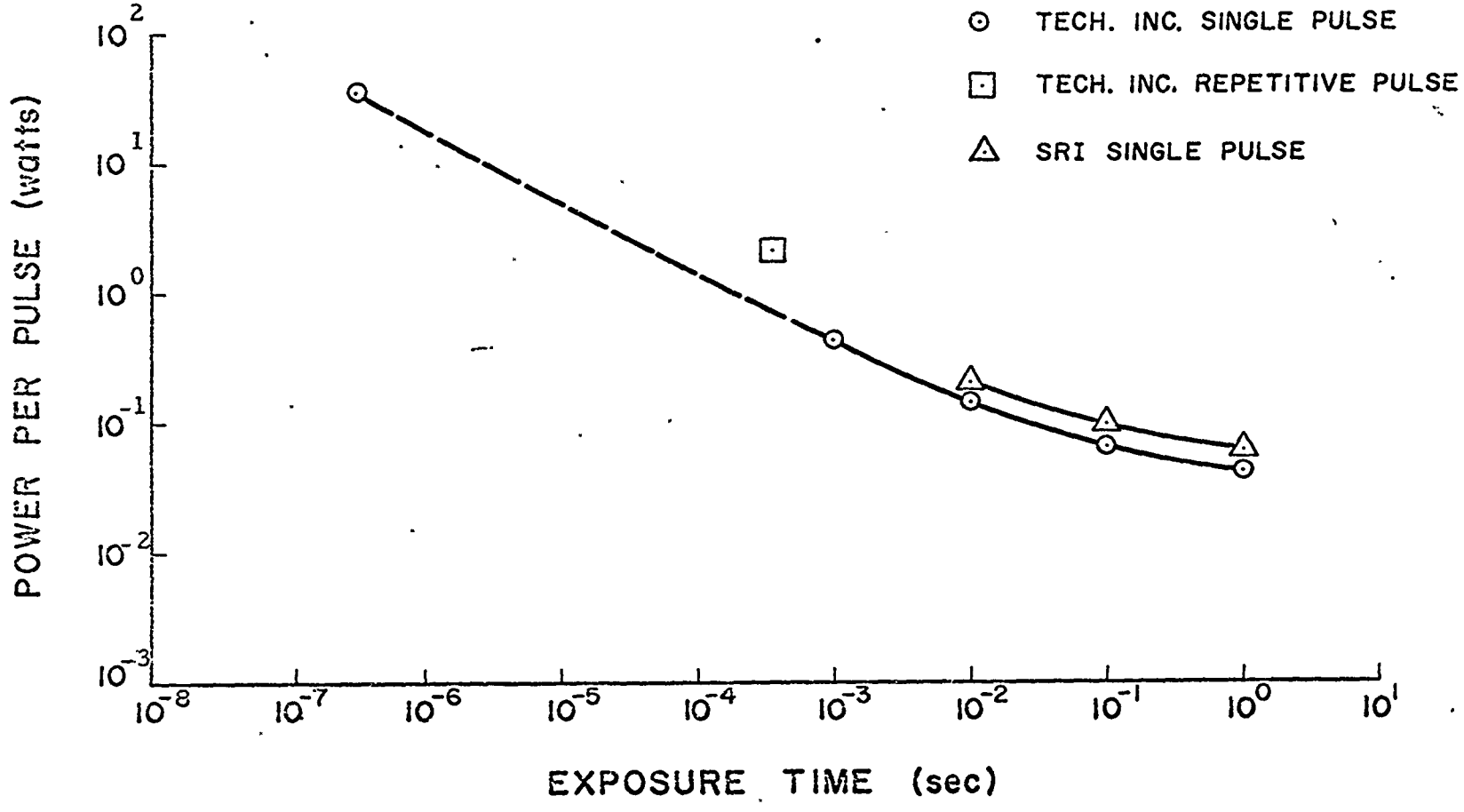

Figure 14. Retinal Burn Threshold versus Exposure Time

Work was done elsewhere[1] using a Nd^{3+}-YAG laser to determine retinal burn thresholds for primates with some exposure durations being on the same interval as that reported in this document. The results obtained[1] were plotted (SRI curve) as shown in Figure 14. The results[1] are consistently higher than the results for the single pulse exposure reported here by a factor of approximately 1.2. No remark was made about the modal pattern of the laser beam used;[1] and, if this modal pattern was not TEM_{00}, then it is to be expected that the thresholds would be higher because this beam would have a larger divergence.

In work reported elsewhere[11], an argon-ion laser operating in the TEM_{00} mode was used to produce retinal burns. The retinal burn thresholds for primates irradiated by this argon-ion laser fall along a straight line when displayed in a log-log plot. The reason why the Nd^{3+}-YAG data are non-linear and the argon-ion laser data are linear on the log-log plots is not known.

The retinal burn thresholds reported in this document for the Nd^{3+}-YAG laser are approximately a factor of 7 larger than those obtained[11] with the argon-ion laser for the same pulse durations. This value of 7 is approximately equal to the product of the ratio of the absorptance of the fundus[12] at 514.5 nm to the absorptance of the fundus at 1060 nm (this factor is 2.5) and the relative areas of the minimum spot areas for these two lasers

(this factor is 2.89 as seen below). The divergence of the Nd^{-3}-YAG laser beam is a factor of 1.7 larger than the divergence of the argon-ion laser beam[11]. Thus the minimal area of the spot of the argon-ion light on the fundus should be a factor of about 2.89 smaller than the spot area for the YAG laser light. Because of the larger beam divergence and the smaller absorptance of the fundus at 1060 nm, it is to be expected that the retinal burn threshold for the Nd^{3+}-YAG laser would be a factor of 7.2 larger than for the argon-ion laser. The agreement between these two values 7 and 7.2 is remarkable. This can be taken to imply (1) that the Nd^{3+}-YAG results reported here are internally consistent with the argon-ion data reported elsewhere[11] and (2) the absorptance values for rhesus monkey fundus oculi are accurately known -- at least on a relative basis.

The curve in Figure 14 between the 10^{-3} sec and 1 sec exposures can be extrapolated graphically to predict the retinal burn probability for a Q-switched pulse having a FWHMP of 0.7μ sec. This extrapolation was performed over three orders of magnitude in exposure time and it predicted a value of 20 μ J for the retinal burn threshold. The nearness of the extrapolated value to our measured value reveals an internal consistency between the long pulse duration data and the Q-switched data for the Nd^{3+}-YAG laser operated in the TEM_{00} mode.

Results were reported elsewhere[1] for retinal burn thresholds for primates exposed to a Q-switched Nd^{3+}-YAG laser. A value of 150 μ J was reported

there for the retinal burn threshold for the macular region of rhesus monkey eyes using a pulse with a 30 nsec FWHMP. It is clear that this value (150 μ J) is not in agreement with the 24±1μ J value reported in this current work. The exact reason for this apparent disagreement is not fully understood. A 30 nsec pulse would be expected to have an associated lower retinal burn threshold than would a 0.7 μ sec pulse if all other experimental conditions were the same. Clearly, the conditions in these two experiments were not the same. In the former experiment[1], the eyes were uncorrected whereas in the current experiment they were corrected. In the former experiment, the spot diameter into which the radiation was focussed was estimated to be 90μ. In the current experiment, the region into which the energy is focussed is believed to be a "minimal-size-spot" and is estimated to be 40 μ or less in diameter. Finally, the energy distribution in the laser beam in the former experiment was unreported whereas in the current experiment it was known with certainty to be TEM_{00}.

It is worthwhile to compare the value for the threshold power per pulse for the train of 0.7 μ sec pulses at a pulse repetition rate of 1 kHz lasting for 0.5 sec with the value obtained from the single 0.7 μ sec exposures. The former value is 2.1 watts whereas the latter value is 34.3 watts and these differ by a factor of about 17. Making a similar comparison for the results obtained for the power per pulse (15.7 mw) to be reported[13] for a train of 10 μ sec pulses at a pulse repetition rate of 1 kHz lasting for

0.5 sec with the value (157 mw) obtained for single 10 μsec exposures using an argon-ion laser, one finds that these two results differ by a factor of 10. These comparisons reveal what appears to be a cumulative effect for lasers operating in the repetitive pulse mode. This cumulative effect implies that pulses, subthreshold when taken separately, act in concert in the pulse trains to produce lesions in rhesus monkey eyes. Moreover, upon comparing the factor of 17 with the factor of 10, it is concluded that the degree of the cumulative effect may depend upon the FWHMP of the pulses composing the pulse trains. This conclusion is indicated (1) because the pulse repetition rates (1kHz) and the pulse train durations (0.5 sec) were the same for each laser and (2) because the results obtained for the retinal burn thresholds are based on enough observations to make the experiments statistically valid.

Calculations were performed using a straightforward thermal model[14] based on the criterion that a critical temperature[15] must be reached to produce a retinal lesion, in an attempt to predict the experimental results. These retinal burn calculations were performed for exposures to both the single 7×10^{-7} sec pulses and trains of the 7×10^{-7} sec pulses with a pulse repetition rate of 1 kHz lasting for 0.5 sec. The calculations predicted results that agreed very well with the single 7×10^{-7} sec exposures; however, these calculations predicted a cumulative effect for the 1 kHz pulse train which was an order of magnitude smaller than that which was observed experimentally. The reasons for the disagreement between the experimental

and calculate results for the repetitive pulse train is not understood. As seen in another study [13], in which this cumulative effect was observed at several pulse repetition rates, this disagreement is not due to some artifact of the 1 kHz pulse train used. The disagreement between the experimental values and calculated values may indicate either (1) the thermal relaxation time and heat transfer coefficients of the chorioretinal tissues involved are temperature dependent or (2) the optical absorption coefficients of the chorioretinal tissues involved are temperature dependent.

Some remarks about the use of both (1) the probit analysis and the (2) the arithematical average of the individual retinal burn thresholds to determine the ED50 value and/or the P=0.5 values are in order. An underlying assumption for using the probit technique to analyze these data is that the retinal burn/no burn observations are independent ones. This implies that each retinal site irradiated is independent of any other retinal site and corresponds to a random sample of the primate population. It appears that the retinal burn data like that compiled in Table I; for example, from observations on an eye may not be truly independent. To see why these retinal burn probabilities may arise from dependent observations consider the following. Measurements taken elsewhere[1] show that the sensitivity of the chorioretinal tissues to laser light varies by about a factor of 2 in going from the paramacular to the macular region and the latter is the more sensitive than the former. Data from retinal burn thresholds

taken for 30 primate eyes for a given exposure duration, e.g., data like that in Table VII reveal a variation of a factor of as much as 5 or 6 in the sensitivity of the macular region from primate to primate in the rhesus monkey population. If the factor of 5 or 6 is considered to be statistically valid, then the variability between eyes at random is larger than the variability within any particular eye.[1] Hence, it is possible that the frequency of observations used to determine retinal burn probabilities in any energy interval is different than for the population[16]. If this is true, then the observations are not truly independent and the probit technique must be used with caution, if used at all. It is interesting to note that of the 6 sets of 30 primate eyes investigated in this study, only those listed in Table VII reveal retinal burn thresholds with spreads (ratio of highest to lowest values) that are only slightly greater than a factor of 2. It is interesting to note that the mean of the retinal burn thresholds for the 30 eyes in Table VII is 1.70 mJ with a standard deviation, σ, of 0.79mJ. The two values in Table VII which cause the spread to be greater than the factor of 2 mentioned above have deviations from the mean value larger than 3σ. Following good statistical analysis procedures, some statisticians recommend excluding measurements with deviations from the mean which are greater than 3σ. If this procedure is followed with the data in Table VII, then the most probable value obtained for the retinal burn threshold is (1.50 ± 0.16)mJ, and it is concluded that the variations in the sensitivity of the macular region of normal rhesus monkey eyes do not differ

significantly by amounts greater than the factor of 2 from primate to primate. It this is the case, then the conditions for use of the probit analysis may be satisfied.

As mentioned previously in this report it was the apparent difficulty using the probit analysis that led to the determination of the ED50 values by computation of the arithmetical average for the set of 30 eyes irradiated by the laser for a given exposure duration. It is observed that the ED50 values obtained using the probit analysis and determined by the averaging techniques agree well statistically. Moreover, it is noted that the 95% confidence limit intervals obtained are smaller for the probit analysis than for the averaging process. The reason for the lack of agreement of the 95% confidence limit intervals using these two techniques is not known; but, it is suggestive of the fact that more observations are being used in the probit analysis than in the averaging process.

Finally, it is observed, from Figure 14, that there is dearth of experimental data available for lasers operating in the near infrared in the TEM_{00} mode. For these conditions, there are no retinal burn threshold data for (1) single pulses shorter than 7×10^{-7} sec, (2) single pulses having durations from 10^{-6} sec to 10^{-3} sec, (3) single pulses having durations longer than 1 sec and (4) repetitive pulse trains other than the one reported in this work.

5. SUMMARY AND CONCLUSIONS

The ocular effects of near infrared laser light were investigated in this study. The laser used during the investigation was a Nd^{3+}-YAG laser. This laser emitted light at a wavelength of 1060 nm in the TEM_{00} mode. Retinal burn probabilities were determined for six different exposure durations. The exposures were for (1) single pulses with durations of 1 sec, 10^{-1} sec, 10^{-2} sec, 10^{-3} sec and 7×10^{-7} sec and (2) a train of 7×10^{-7} sec pulses with a pulse repetition rate of 1 kHz and lasting for 0.5 sec. Retinal burn thresholds were obtained for 30 rhesus monkey eyes for each exposure duration. The ED50 values were determined (1) by using a probit analysis of the retinal burn data and (2) by finding the arithmetical average of the retinal burn thresholds for each set of 30 primate eyes. The arithmetical averaging technique was employed when it was demonstrated [16] using Monte Carlo methods that the retinal burn observations may not be independent as they must be for accurate use of the probit method [10]. The results obtained from these two analyses are shown in Table XIII with the corresponding 95% confidence intervals. The reasons for the agreement between the ED50 values and the disagreement between the 95% confidence limit intervals for corresponding exposure durations from these two analyses are not understood fully.

The ED50 values obtained for the long pulse exposures (10^{-3} sec to 1 sec) in this study were compared with ED50 values using another Nd^{3+}-YAG laser elsewhere [1]. The ED50 values found in the other study [1] disagreed con-

sistently by a factor of 1.2 with those found in the study reported here. The disagreement between these ED50 values probably indicates that the other Nd^{3+}-YAG laser was not operated in the TEM_{00} mode.

The ED50 value (24±1 μJ) for a single 7×10^{-7} sec pulse was compared with the ED50 value (20 μJ) by extrapolating graphically the long pulse data (10^{-3} sec to 1 sec exposures) on a log-log scale. The closeness of these two values was interpreted to imply that the long pulse data and the single Q-switched pulse data were internally consistent.

The ED50 value (24±μJ) for the single 7×10^{-7} sec pulse was compared with the ED50 value (150μJ) obtained for a 30 nsec pulse in another study[1]. A portion of the disagreement between these two values is attributable to (1) eyes were not corrected in the other study[1] and (2) estimated retinal spot size was 90μ in the other study[1] and 40μ or less in this study.

A cumulative effect was found for the Nd^{3+}-YAG laser operating in the repetitive pulse mode. The existence of this cumulative effect appears obvious from a comparison of the ED50 value (24±1μJ) for single 7×10^{-7} sec exposures with the ED50 value (1.50±0.03μJ) per pulse in the train of 7×10^{-7} sec pulses at a pulse repetition rate of 1kHz lasting for 0.5 sec. The observation of this cumulative effect indicates that subthreshold pulses (taken individually) appear to work in concert (in the pulse trains) to produce retinal lesions. Calculations performed to predict the ED50 values using a straightforward thermal model[14] and a

temperature criterion [15] gave results in agreement with experiments for the single 7×10^{-7} sec exposures; but, these calculations underestimated the cumulative effect observed by about an order-of-magnitude. The reasons for the lack of agreement between the calculations performed and the experimental results obtained for the repetitive pulse train merits further study.

A great lack of retinal burn threshold data exists for lasers operating at near infrared wavelengths. This dearth of information indicates that much additional work must be done to obtain ED-50 values for single pulse exposures and many different pulse trains. The single pulse studies should include exposure durations (1) shorter than 7×10^{-7} sec., (2) between 10^{-6} sec and 10^{-3} sec., and (3) longer than 1 sec. The pulse train experiments that appear to be required include (1) trains composed of pulses with several different FWHMP, (2) trains with many different pulse repetition rates and (3) pulse trains with several different durations.

6. REFERENCES

1. A. Vassiliadis, R. C. Rosan and H. C. Zweng. "Research on Ocular Laser Thresholds", Final Report Contract F41609-68-C-0041, August 1969.

2. A. M. Clarke. "Ocular Hazards" (Handbook of Lasers with Selected Data on Optical Technology, Robert J. Pressley, Ed.) Chemical Rubber, Co., Cleveland, Ohio, 1971, Page 3-10.

3. D. H. Sliney. "The Development of Laser Safety Criteria-Biological Considerations" (Laser Applications in Medicine and Biology, Volume I, M. L. Wolbarsht, Ed.), Plenum Press, New York 1971, Page 163-238.

4. A. Vassiliadis. "Ocular Damage from Laser Radiation" (Laser Applications in Medicine and Biology, Volume I, M. L. Wolbarsht, Ed.), Plenum Press, New York 1971, Page 125-162.

5. R. G. Allen, et al. "Research on Ocular Effects Produced by Thermal Radiation", Final Report, USAF Contract No. AF41(609)-3099, July 1967.

6. R. G. King and W. J. Geeraets. "The Effect of Q-Switched Ruby Laser on Retinal Pigment Epithelium in Vitro", Acta Ophthal. 46, 617 (1968).

7. Herwig Kogelnik. "Modes in Optical Resonators", (Lasers, Volume I, Albert K. Levine, Ed.) Marcel Dekker, Inc., New York, 1966, Pages 295-347.

8. G. Wald and D. R. Griffin. "Change in Refractive Power of Human Eye in Dim and Bright Light", J. Opt. Soc. Am., 37, 321 (1947).

9. R. E. Bedford and G. Wyszecki. "Axial Chromatic Aberration of the Human Eye", J. Opt. Soc. Am., 47, 564 (1957).

10. D. J. Finney. Probit Analysis, Second Edition, Cambridge University Press, New York, New York, 1952.

11. G. H. Bresnick, et al. "Ocular Effects of Argon Laser Radiation", Investigative Ophthalmology 9, 901 (1970).

12. W. J. Geeraets and E. R. Berry. "Ocular Spectral Characteristics as Related to Hazards from Laser and Other Light Sources", Amer. J. Ophthal. 66, 15 (1968).

13. C. H. Skeen, W. Robert Bruce, J. H. Tips, Jr., M. G. Smith and G. G. Garza. "Ocular Effects of Repetitive Laser Pulses", Contract No. F41609-71-C-0018, Draft Final Report, to be submitted on 30 April 1972.

14. M. Mainster, T. J. White, J. H. Tips and P. W. Wilson. "Retinal Temperature Increases Produced by Intense Light Sources" J. Opt. Soc. Am. 60, 264(1970).

15. M. Mainster. "Destructive Light Adaptation" Ann. of Ophthal. 2, 44 (1970).

16. Richrad McNee. A Private Communication.

17. G. Birnbaum. "Optical Masers" Academic Press, New York, 1964 page 68.

18. A. Goldstein. "Biostatistics" MacMillian Co., New York, 1964, Page 177.

APPENDIX A

The Nd^{3+}-YAG Laser System

A schematic diagram of the YAG laser is shown in Figure 15. To describe the YAG system, a light ray was considered as passing through the laser cavity beginning at the 100% reflector on the left. From this dielectric coated glass substrate, the ray travelled to the quartz crystal modulator and then passed through the Nd^{3+}-YAG rod where it was amplified. It then went through the spatial filter with the 2.0 mm diameter aperture to the dielectric coated output mirror on the right.

The laser rod was pumped by two halogen-tungsten cycle flood lamps which were rated at 3 kw electrical. The rod and the lamps were mounted in a gold plated cavity in the "close-wrapped" configuration.

The maximum cw output power of this laser was 13 watts when the spatial filter was removed from the cavity. When the spatial filter was removed, the output beam was multi-mode; and, when using a thermal imaging screen as described later herein, the "mode-hopping" characteristic of this type of output was observed. With the spatial filter in place, all modes except the TEM_{00} were suppressed. The maximum cw power output for the TEM_{00} mode was 2.4 watts.

When the cavity was configured as shown in Figure 15 and a 25 megacycle

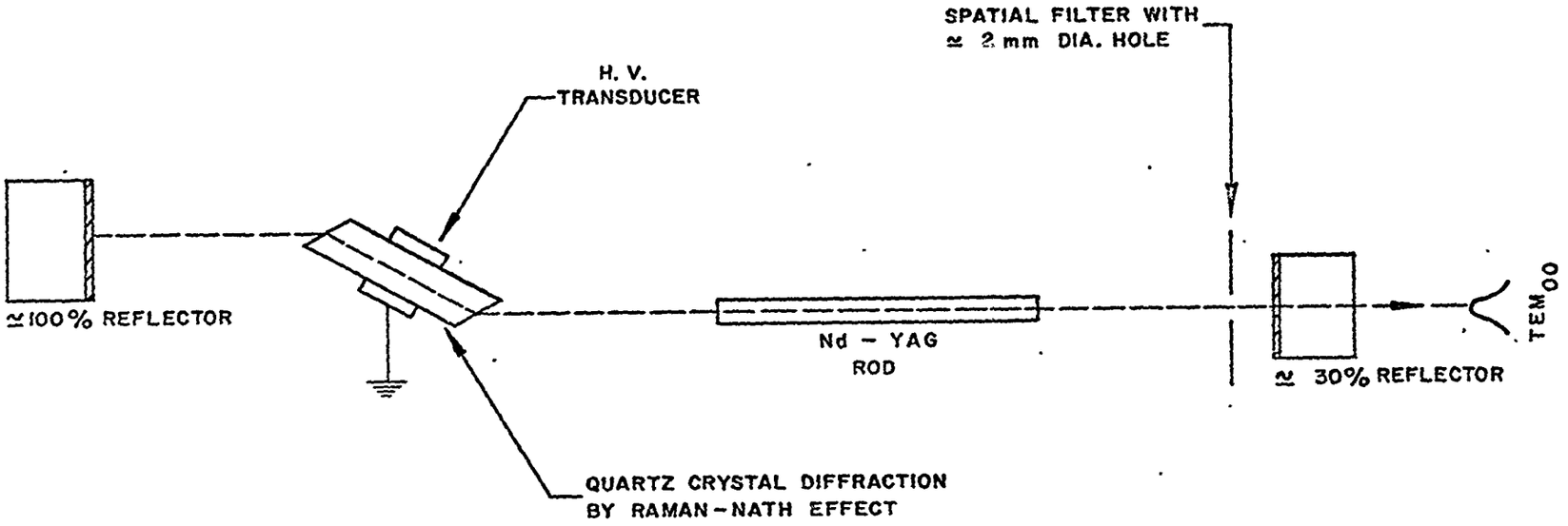

Figure 15. A Schematic Diagram of the Nd^{3+}-YAG Laser Cavity

electromagnetic field was applied to the quartz crystal, all laser activity was suppressed. This suppression was obtained by the large increase in the diffraction losses of the cavity when the crystal was activated in this manner. The crystal behaved like a diffraction grating via the Raman-Nath effect. This crystal was used as a Q-switch. It was used to keep the laser cavity losses high while energy was being stored in the rod. Then the cavity losses were minimized by gating the R-F off the crystal and the stored energy was released in a giant pulse. The FWHMP of the pulses was 500 ns and they had a peak of 6 kw. The R-F to the Q-switch was controlled internally so that either a single pulse or a train of the pulses with pulse repetition frequencies from 0.5 kHz to 50 kHz were obtained. External triggering was used to obtain a pulse repetition rate from 1Hz to 50 kHz.

Laser Beam Modal Pattern

It was necessary to be assured that the 1060 nm beam is in the TEM_{00} mode to perform the retinal irradiations. To be assured the 1060 nm beam was TEM_{00}, the following was considered. According to the manufacturer the Nd^{3+}-YAG laser system was designed to operate in the TEM_{00} mode when the spatial filter shown in Figure 15 was in place and properly alined. The mirror configuration of the Nd^{3+}-YAG system consisted of a concave spherical reflector having a radius, R, of 500 cm and a plane output mirror in a laser cavity having a length, d, of 58 cm. The g(g=1-2d/R) parameter, of this cavity is 0.77 and the limiting aperture, a, is

0.15 cm. The Fresnel number, N, was given by the expression $N=a^2/2\lambda d$ where λ was the wavelength of the laser light and, a and d were as defined previously. Using these numbers, the power loss per transit for the TEM_{00} mode was estimated approximately 40% whereas for the TEM_{01} mode it is 5db. There is not sufficient gain in the Coherent Radiation Incorporated Model 60 YAG laser system to sustain lasing at such high loss and so one can conclude that the possibility of either the TEM_{01} or of higher order modes of operation of this sytem is highly unlikely.

Eventhough it is not likely according to the theoretical analysis for this system to have any modes present except the TEM_{00}, it is considered wise to make some experimental observations to give assurance that this is the case. To accomplish this, the arrangement shown in Figure 16 is used. The laser is tuned so that it should be operating in the TEM_{00} mode. The output beam is allowed to impinge upon a thermal imaging screen. The light emitted by this screen at, S, has a star-like appearance. The center of this star-like pattern obtained when visible laser light in the TEM_{00} mode is reflected from a surface.

An additional visual observation is performed. The laser beam is diverged by a lens, L, and the pattern observed at the thermal imaging screen. It has the appearance shown at, Y, in Figure 16. This appears essentially the same as photographs taken elsewhere [17] of the beam of a laser operating in the TEM_{00} mode. Moreover, there is no apparent fluctuation in this pattern

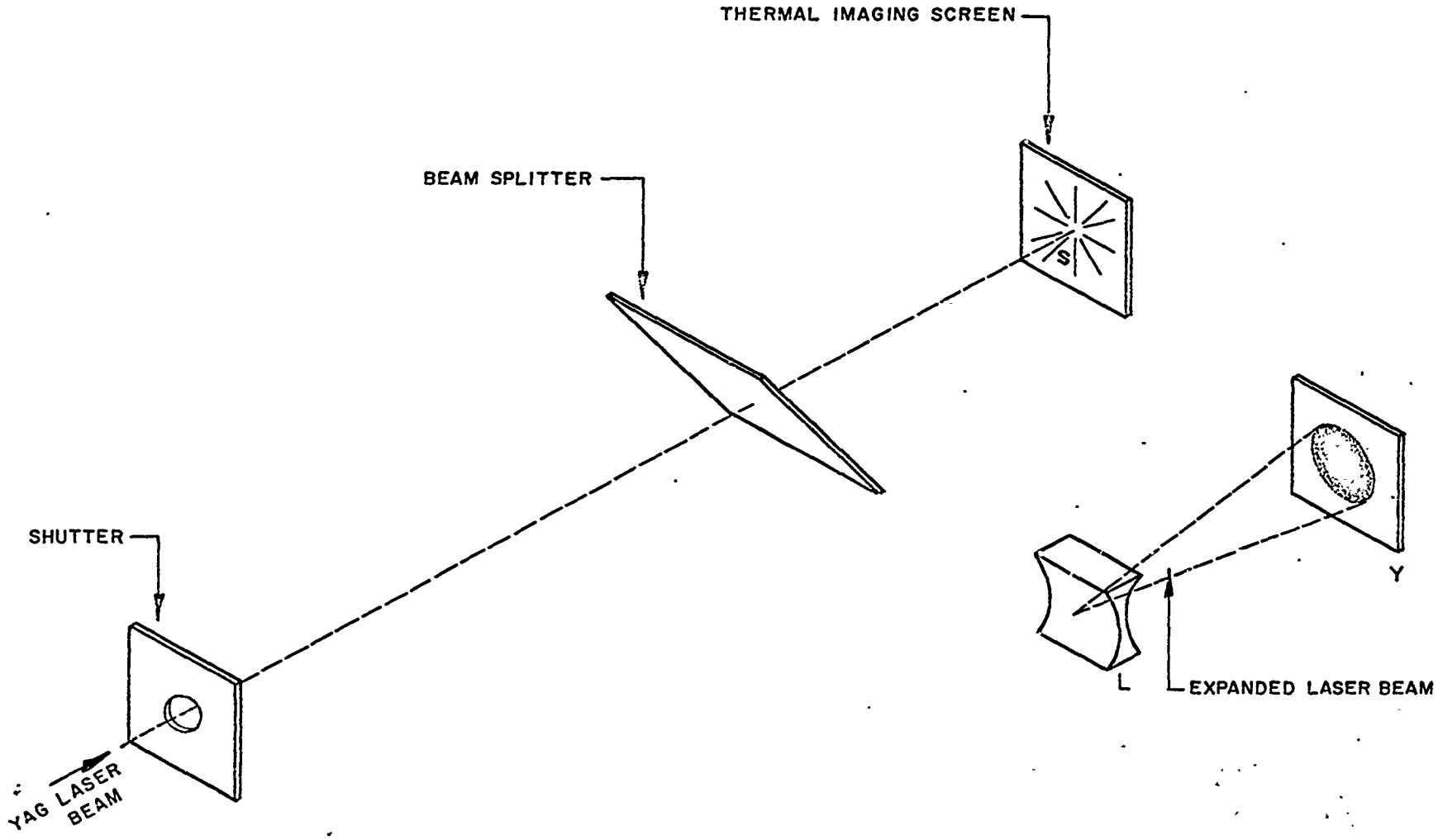

Figure 16. Diagram Showing Use of Thermal Imaging Screen to Observe TEM_{00} Mode Pattern.

with time. This lack of fluctuations is unlike that observed when the multiple mode beam impinged upon the thermal imaging screen. In this latter situation, fluctuations appear and these are due to "mode-hopping".

The observations of the modal pattern with the thermal imaging screen in conjunction with the theoretical analysis gives sufficient assurance that the laser is operated in the TEM_{00} mode during the experiments. It is considered unnecessary to perform more complicated measurements regarding the energy distribution in the laser beam. Two additional techniques that might be used are: (1) expansion of the laser beam with a lens and scanning this expanded pattern with an array of photodiodes and (2) beam splitting and heterodyning the beam segments against themselves and looking for beat frequencies between the TEM_{00} mode and off-axis modes on a spectrum analyzer.

For the irradiations of primate eyes to be performed properly, it is necessary to know that the 1060 nm light will impinge on a selected retinal site. To be assured that the light would be impinged on the selected sites, laser beam aiming experiments were performed. The arrangement used for these aiming experiments is shown schematically in Figure 17. A source having considerable ultraviolet light was used to irradiate the thermal imaging screen. This light co-illuminated the thermal imaging screen with the light of an ophthalmoscope (this light has cross-hairs intersecting at its center). The aligned laser system was operated and the beam aimed at the cross-hair intersection when the screen was in the near field (about 5 cm from the "pop-up" mirror and in the far field

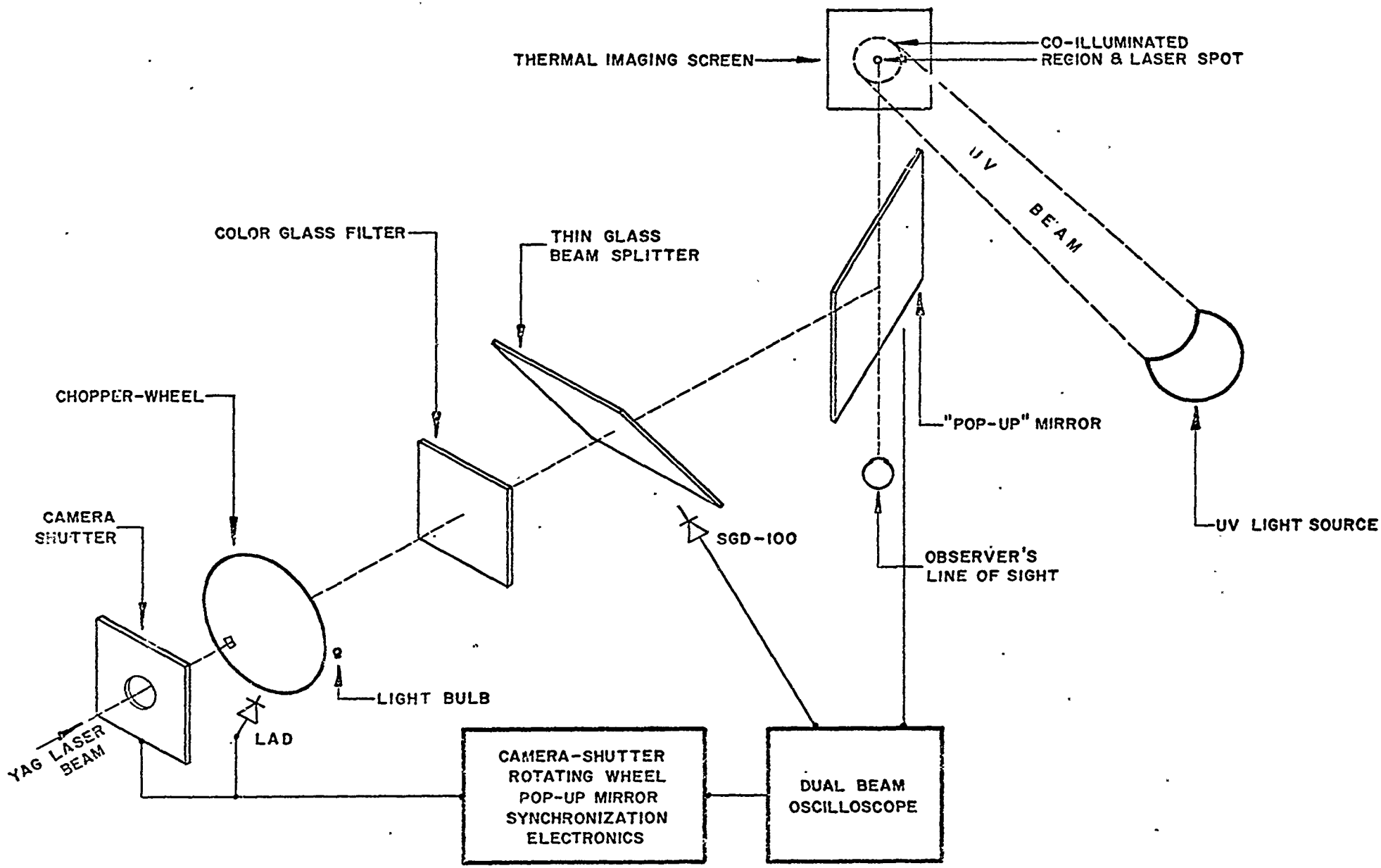

Fig. 17. Schematic Diagram of Arrangement Used in Laser Beam Aiming Experiments.

(about 50 cm from the "pop-up" mirror). The laser beam impinged upon the screen at a given position and this position relative to the intersection of the cross-hairs was noted. Adjustments in the laser beam direction were made until the intersection of the cross-hairs and the spot on which the laser beam impinged were identical. Clearly this technique revealed that the laser beam can be aimed precisely at the selected retinal location. These aiming experiments were performed routinely throughout the retinal burn program.

APPENDIX B

Laser Energy Detection and Calibrations

A camera shutter was used to obtain the pulses with FWHMP's of 10^{-1} sec and 1 sec. A schematic diagram of the arrangement used with the shutter is shown in Figure 18. The shutter used was the Uniblitz model 26-A having an opening-closing time that was continuously variable from 1.5 msec to 9.99 sec. The opening-closing time was obtained using the Uniblitz model 300 electronic controller unit. The action of this shutter was synchronized electronically with the emplacement of the "pop-up" mirror. The "pop-up" mirror turned into place, then the shutter was activated causing the pulse of the laser light of the desired duration to impinge upon the cornea of the primate under experimental observation.

The combination of a camera shutter and a rotating-slotted-wheel was used to obtain the 10^{-3} sec, 10^{-2} sec, and 10^{-1} sec duration pulses. The experimental arrangement used to obtain these pulses is shown in Figure 19. The rotating-wheel was opaque to the laser light except at a slit cut near its periphery. The length of the slit and the angular velocity of the wheel were controlled to obtain the desired duration of the laser light pulse. The opening and closing of the camera shutter was synchronized opto-electronically with the position of the slit so as to be open while the slit was passing and to be closed after its passage and before it can return so that only one pulse

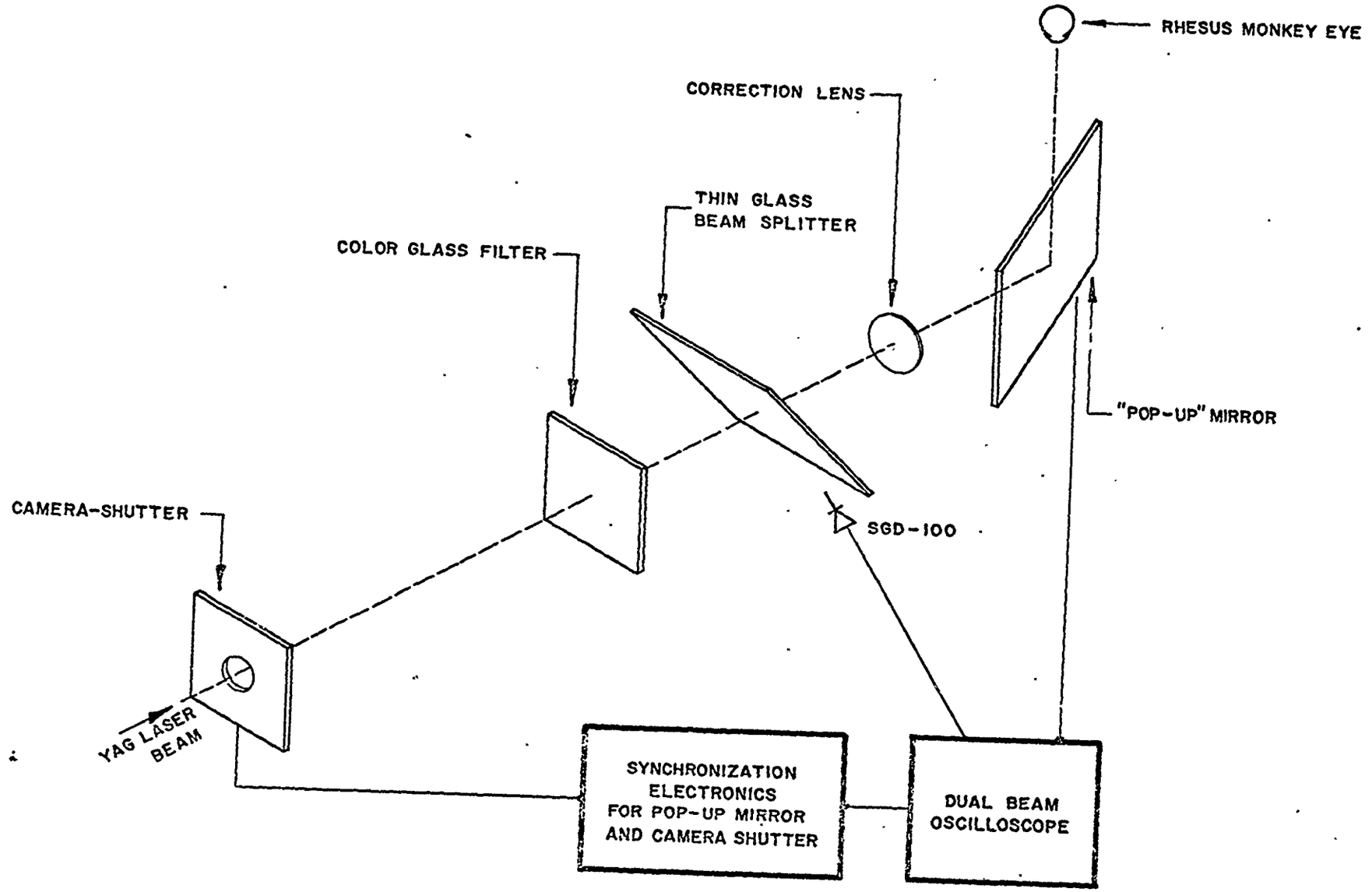

Fig. 18. Schematic Diagram Showing Use of Camera Shutter to Obtain Laser Pulses.

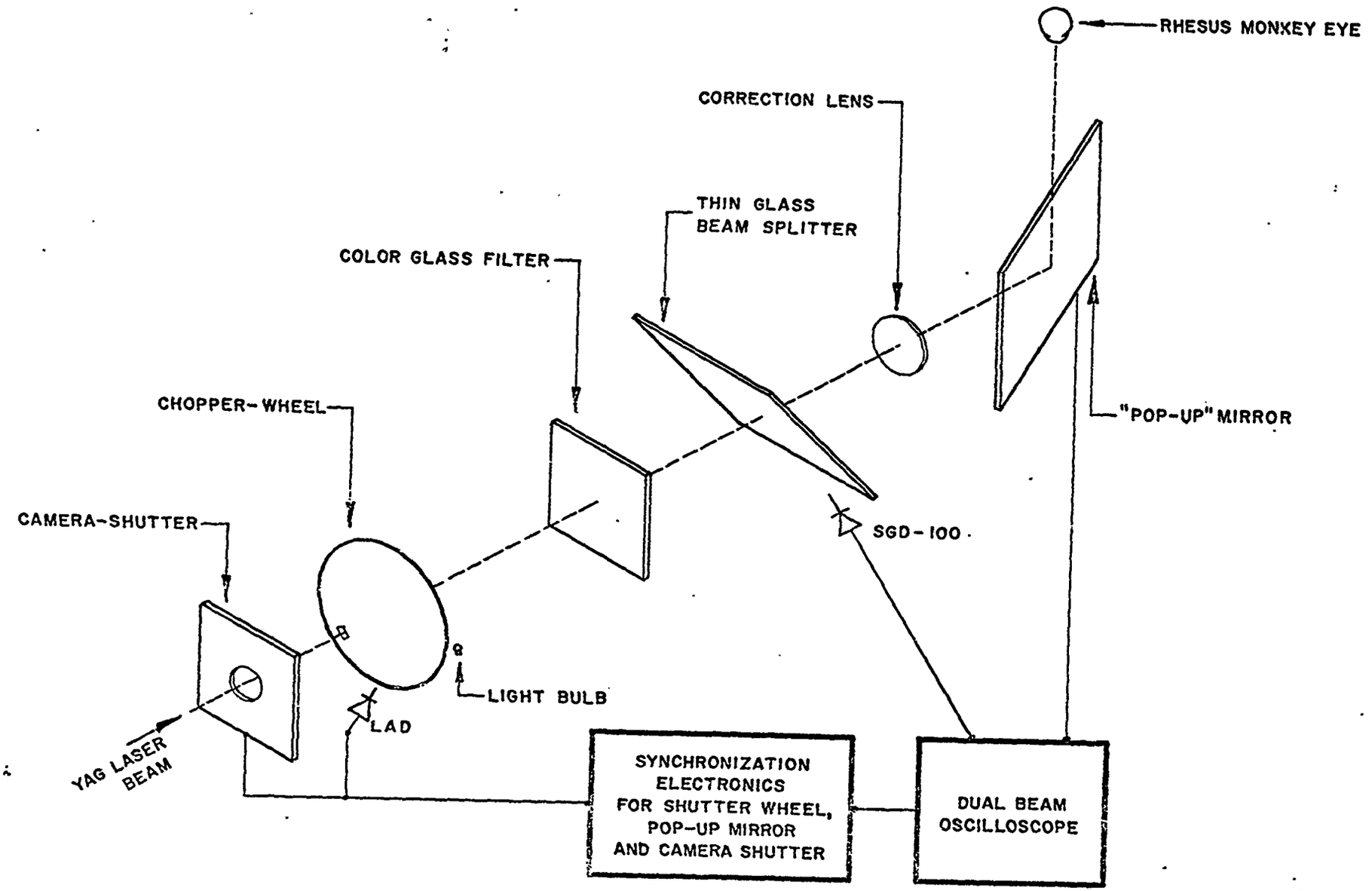

Fig. 19. Schematic Diagram of Experimental Arrangement for Use of Camera-Shutter, Rotating-Wheel Combination to Obtain Laser Pulses.

was obtained. The synchronization was accomplished by using a light activated photodiode (LAD) to detect the light passing through the slit from a light bulb and by using the necessary electronic delay circuitry. The laser pulse widths were quite reproducible because the angular velocity of the wheel is very uniform.

The methods for obtaining the single Q-switched pulses and the trains of the Q-switched pulses were described adequately in Appendix A and will not be repeated here.

In the determination of the retinal burn threshold, the energy per laser pulse was a key parameter to be measured. This energy was determined for every irradiation of a primate eye. Two instruments with calibrations traceable to the National Bureau of Standards were used to measure the laser power and the energy in an absolute manner. The placement of these for the experiments is shown schematically in Figure 20. One of these was a Coherent Radiation Incorporated Model 201 power meter and the other was a HADRON/TRG model 100 ballistic thermopile. The power meter was a device for measuring the power in cw laser beams. The ballistic thermopile was a detector for measuring the energy in laser pulses. Each of these had an accuracy of $\pm$ 5%.

The response of the power meter was so slow that it is not capable of measuring either the power or the energy in the 1 sec and shorter laser

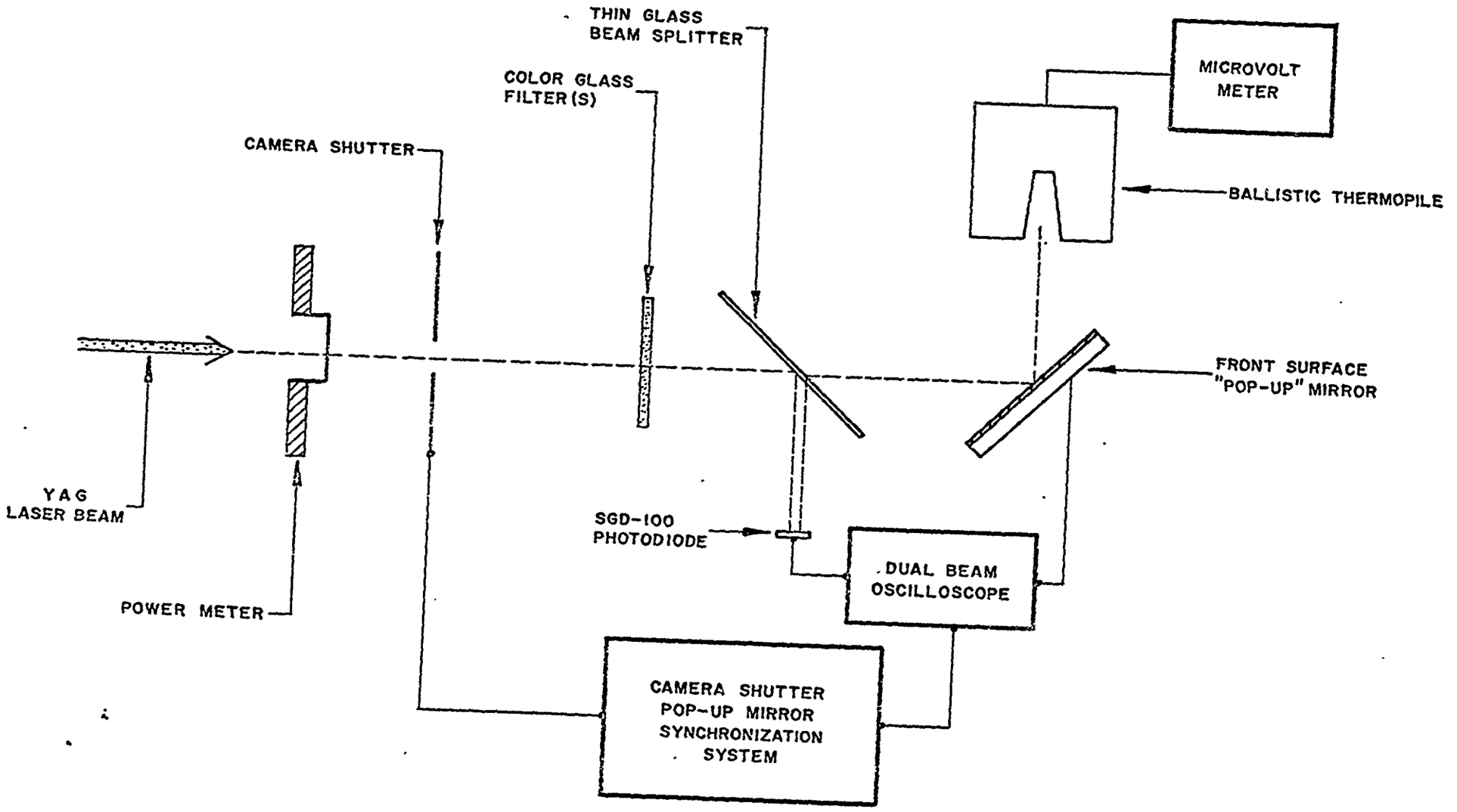

Fig. 20. Schematic Diagram of Arrangement to Determine the Power and the Energy for the Laser Pulses.

pulses of interest in this study. The ballistic thermopile was capable of measuring laser pulse energy provided it was delivered in 5 sec or less and the energy was large enough. The ballistic thermopile had a sensitivity of 198 μv/J and detected a pulse energy as large as 150J and as low as 1.5×10^{-3} J. Many of the pulses of interest had considerably less energy than 1.5×10^{-3} J; hence, it was necessary to use another detector to determine the energy of each pulse.

To determine the energy for each laser pulse it was necessary initially to use a silicon photodiode. The photodiode used is the EG&G model SGD-100, silicon photodiode. The laser was operated in the chopped-pulse mode and the response of the diode in the form of the instantaneous pulse power and the time integral of this instantaneous pulse power were displayed on the Tektronix model 555 dual beam oscilloscope. The energy of the pulses was measured simultaneously using the ballistic thermopile. In this manner it was possible to calibrate both the pulse height (peak power) and the total integrated power (pulse energy) from the diode-scope responses versus the ballistic thermopile measurements. This procedure was followed throughout the irradiations made using laser pulses having a 1 sec duration. During these irradiations using the 1 sec duration laser pulses, the power meter was placed in the laser beam at the exit mirror (see Figure 20) and the power recorded before and after the irradiations. This power determination in conjunction with the pulse duration observation permitted another determination of the pulse energy by multiplying the power by the pulse duration. It

was found that this latter determination of the pulse energy was just as reliable or better than the value obtained using the pulse height or the time integral of the instantaneous power. This latter technique was used for the 10^{-3} sec, 10^{-2} sec and 10^{-1} sec irradiations of the primate corneas with the laser pulses.

Throughout the irradiations, it was necessary to use optical attenuators in conjunction with changing the laser pump energy to vary the energy of a pulse incident on the primate corneas. These attenuators were calibrated daily by determining their external transmissions. The energy of the 7×10^{-7} sec pulses and the energy per pulse in a train of the 7×10^{-7} sec pulses were determined in the following manner.

The Nd^{3+}-YAG laser was operated in the Q-switched mode. The Q-switch controller-box was governed internally to give a continuous train of the Q-switched pulses with a pulse repetition rate of 1 kHz. The FWHMP of these pulses was determined and shown to be 0.7 μsec. The average power of this pulse train was monitored then with the Coherent Radiation Incorporated model 201 meter. This average power was readily converted into the energy per pulse since the pulse repetition frequency was known.

The Q-switch function control box was governed then, in the external-trigger-mode, using a pulse train and a waveform generator. This arrangement made it possible to select trains of the 0.7 μsec pulses having a pulse

repetition rate of 1 kHz and lasting for 0.5 sec. These individual pulse trains were detected with the HADRON/TRG model 100 ballistic thermopile. The energy per pulse was determined readily from the sensitivity of the ballistic thermopile, the pulse repetition rate and the pulse train duration.

Comparison of the pulse energies determined by these two independent and absolute detectors agreed with each other within the $\pm$ 5% accuracy of the two instruments.

With the energy per pulse known, it was possible then to calibrate the response, in volts, of the SGD-100 photodiode to the laser light pulses in terms of the energy per pulse. This calibration was performed routinely throughout the experiments. Thus it was possible to determine the energy per pulse for each and every irradiation of a primate eye with the Q-switched laser pulses and this was done.

APPENDIX C

Statistical Analyses of Data

One analysis was performed according to the method described by Finney[10] except that the weighting coefficients and working probits were calculated from formulas instead of being selected from tables. All calculations were performed automatically by a Wang 700 programmable calculator. The graphical plot of the data was generated automatically from the resulting parameters by means of a Wang 702 plotting output writer operating in conjunction with the calculator.

The data for a typical probit analysis consist of a set of energy bands $\{[e_i, e_{i+1}]\}$ together with the number of burns, n_i, and the number of trials, N_i, in each band. The lowest energy band $[e_0, e_1]$ used in the analysis is usually the highest for which there are no burns at energies below e_1. The highest band used $[e_M, e_{M+1}]$ is normally the lowest for which there are 100% burns at energies above e_M. Each energy band is actually represented for analysis purposes by the energy at the midpoint: $E_i = \frac{1}{2}(e_i + e_{i+1})$ for $i = 0, 1, 2, \ldots, M$.

Probit analysis begins with the assumption that the burn probabilities, $p_i = n_i/N_i$, are approximately normally distributed with respect to either the energies or the logarithms of the energies. The logarithms are generally to be preferred since they have the doubly infinite range $(-\infty, \infty)$

which is the proper domain of the normal (gaussian) distribution function. For an appropriately restricted domain, however, the energies themselves may provide a distribution of probabilities more nearly normal, according to the chi-square statistic, than for their logarithms; in which case the choice is problematical. In either case the domain is represented in the analysis by $x_i = (\log E_i \text{ or } E_i)$ for $i = 0, 1, 2, \ldots, M$.

The normal distribution of x, with mean μ and standard deviation σ, is given by

$$P_i = P\{x \le x_i\} = \frac{1}{\sqrt{2\pi}} \int_{-\infty}^{(x_i-\mu)/\sigma} e^{-y^2/2}\, dy$$

(distribution function)

The upper limit of integration is called a probit. A probit is customarily defined as 5 more than $(x-\mu)/\sigma$, which is called a normal equivalent deviate (NED). Probits thus simplify hand calculations by being positive in all but 3 cases out of ten million. Positive probits are neither necessary, practical, nor desirable for automatic machine computation. Therefore, in this paper probit = NED. This probit is seen to be a linear function of x. Therefore, the probit Y_i corresponding to x_i is

$$Y_i = \alpha + \beta x_i$$

where $\alpha = -\mu/\sigma$ and $\beta = 1/\sigma$. The parameters α and β are initially estimated and then improved by iteration of the following algorithm:

1. Calculate Y_i and P_i;
2. Adjust Y_i to a value y_i corresponding to p_i;
3. Apply weighted linear regression analysis to $y_i = \alpha + \beta x_i$ to find new values for α and β.

Adjustment of the probits is accomplished by making use of the facts that

$$\frac{dP}{dy} = Z(y) = \frac{1}{\sqrt{2\pi}} e^{-\frac{1}{2}y^2} \quad \text{(density function)}$$

and

$$\frac{p_i - P_i}{y_i - Y_i} = \frac{\Delta P}{\Delta Y} \doteq \frac{dP_i}{dy} = Z(Y_i) = Z_i.$$

Therefore, $y_i = Y_i + (p_i - P_i)/Z_i$ is the appropriate adjustment.

Weights to be appended at each point, (x_i, y_i), for the regression analysis have been derived by means of the maximum liklihood method[18]. Combining these with the "natural" weights, i.e. the number of trials in each of the associated energy bands, yields the effective weights

$$w_i = \frac{N_i Z_i^2}{P_i(1-P_i)}$$

The parameters α and β are calculated as the solution of the normal equations

$$\alpha \Sigma w + \beta \Sigma wx = \Sigma wy$$

$$\alpha \Sigma wx + \beta \Sigma wx^2 = \Sigma wxy$$

where all summations are over i, i = 0, 1, 2, ... M, and subscripts are implied by the sigmas. The solution is

$$\beta = \frac{\Sigma w \Sigma wyz - \Sigma wx \Sigma wy}{\Sigma w \Sigma wx^2 - (\Sigma wx)^2}$$

$$\alpha = \frac{\Sigma wy}{\Sigma w} - \beta \frac{\Sigma wx}{\Sigma w} = \bar{y} - \beta \bar{x}.$$

The sequences $\{\alpha_k\}$ and $\{\beta_k\}$, produced by repetition of the foregoing algorithm, are not conveniently useful for deciding when to terminate the iterations. The sequence of functions $\{f_k : f_k(x) = \alpha_k + \beta_k x\}$ can, however be used easily for testing the goodness of fit of the n_i to their expected values by means of the chi-square statistic. Since $Y_i = f_k(x_i)$, for any particular k, and $P_i = P(Y_i)$, the expected value of n_i is $N_i P_i$. Chi-square is calculated[18] by

$$\chi^2 = \sum_{i=0}^{M} \frac{(N_i P_i - n_i)^2}{N_i P_i (1 - P_i)}$$

and the algorithm is terminated when this quantity is stabilized to three decimal places.

The mean value of x is that value, μ, for which $y = \alpha + \beta\mu = 0$, or $\mu = \alpha/\beta$. The median effective energy (dose) for producing a burn is

$$ED50 = \begin{cases} \mu & \text{if } x = E \\ 10\mu & \text{if } x = \log E \end{cases}$$

and the 95% confidence limits are obtained from

$$\mu + \frac{(\mu - \bar{x})G}{1 - G} \pm \frac{1.96}{\beta(1-G)} \sqrt{\frac{1 - G}{\Sigma w} + \frac{(\mu - \bar{x})^2}{\Delta}},$$

where $$G = (1.96)^2/(\beta^2\Delta)$$

and $$\Delta = \Sigma wx^2 - (\Sigma wx)^2/\Sigma w,$$

the conversion for $x = \log E$ being obvious.

Three distribution functions were tested in place of the gaussian both to verify the results of the analysis and to determine a possible preference for one of these alternative distributions. The three functions and their associated densities are given in Table XV.

In only two of eight cases for which the tests were made did the gaussian fit the data best according to the chi-square statistic. The logistic distribution had the smallest χ^2 in half the cases and the arctangent distribution led in the remaining two.

Since no clear preference was indicated by the chi-square test, the confidence limits predicted by each distribution were compared. The sine transformation indicated the narrowest confidence interval in five of the eight cases, arctangent in two, and logistic in one. Although the gaussian never predicted the smallest confidence band, the difference between it and the smallest never exceeded four percentage points and the average difference

Table XV. ALTERNATIVE DISTRIBUTIONS

Name	Distribution Function (P)	Density Function (Z)
Logistic	$(1+e^{-y})^{-1}$	$(e^{-y})(1+e^{-y})^{-2}$
Arctangent	$\frac{1}{2} + \frac{1}{\pi}$ Arctan y	$\frac{1}{\pi(1+y^2)}$
Sine	$\frac{1}{2}(1+\sin y)$, $-\frac{\pi}{2} < y < \frac{\pi}{2}$	$\frac{1}{2}\cos y$

was less than two percent. Furthermore, the difference between means was only about 1.6%, clearly within the bounds of experimental error.

In summary, the three alternative distributions do indeed verify the results of the probit analysis but do not indicate any preference for one of these over the gaussian.

The data for the retinal burn thresholds were shown to be normally distributed; therefore, a statistical analysis was performed on the retinal burn thresholds. This analysis involved determining the mean retinal burn threshold, $\bar{X}$, for irradiations by the radiation from a laser operating in a given condition (single or repetitive pulse). The standard deviation, σ, was then determined. The 95% confidence interval was computed using the equation $\bar{X} - 1.96\,\sigma/\sqrt{n} \leq \bar{X} \leq \bar{X} + 1.96\,\sigma/\sqrt{n}$ where n was the number of eyes used to determine $\bar{X}$. The 30 eyes used for every laser operating condition was a practical number from the amount of time necessary to make measurements and obtaining valid results. Thirty observations is sufficient to yield statistically valid results. Since the precision in determining, $\bar{X}$, varies inversely as the $\sqrt{n}$, it would be impractical from time and cost considerations to increase the precision. For the precision to be increased by a factor of ten would require retinal burn threshold data from 3,000 eyes for radiation from a laser in a given operating condition.